REPORT DOCUMENTATION PAGE

AFRL-SR-BL-TR-01-

0266

1. AGENCY USE ONLY *(Leave blank)*	2. REPORT DATE	3. REPORT TYPE AND DATES COVERED
	July 2001	FINAL TECHNICAL REPORT 1 Jul 00 - 31 Mar 01

4. TITLE AND SUBTITLE
POST STALL FLOW CONTROL OVER SWEPT WINGS

5. FUNDING NUMBERS
F49620-00-1-0335

2302/CX
61102F

6. AUTHOR(S)
DEMETRI TELIONIS

7. PERFORMING ORGANIZATION NAME(S) AND ADDRESS(ES)
VIRGINIA POLYTECHNIC INSTITUTE AND STATE UNIVERSITY
BLACKSBURG, VA 24060

8. PERFORMING ORGANIZATION REPORT NUMBER

9. SPONSORING/MONITORING AGENCY NAME(S) AND ADDRESS(ES)
AIR FORCE OFFICE OF SCIENTIFIC RESEARCH
801 N. RANDOLPH STREET, ROOM 732
ARLINGTON, VA 22203-1977

10. SPONSORING/MONITORING AGENCY REPORT NUMBER

11. SUPPLEMENTARY NOTES

12a. DISTRIBUTION AVAILABILITY STATEMENT
APPROVED FOR PUBLIC RELEASE, DISTRIBUTION IS UNLIMITED

12b. DISTRIBUTION CODE

13. ABSTRACT *(Maximum 200 words)*

An experimental study of active control of fully separated flow over a symmetrical circular-arc wing at high angles of attach was performed. The wing was swept at angles up to 45 degrees. The experiments were carried out in a low-speed, open-circuit wind tunnel. Angles of attack from 10 to 40 degrees were tested. The actuation was provided by the periodic oscillation of a 4-percent-chord flap placed on the suction side of the airfoil and facing the sharp edge. Pressure measurements over the wing show that the control increased the normal force coefficient by up to 50%. But the effectiveness of the method decreased with the angle of sweep. The application of flow control on sharp-edged aircraft wings could lead to improved maneuverability, innovative flight control and aircraft weight reduction.

20020118 075

14. SUBJECT TERMS	15. NUMBER OF PAGES
	35
	16. PRICE CODE

17. SECURITY CLASSIFICATION OF REPORT	18. SECURITY CLASSIFICATION OF THIS PAGE	19. SECURITY CLASSIFICATION OF ABSTRACT	20. LIMITATION OF ABSTRACT
U	U	U	

FINAL REPORT ON

Post Stall Flow Control Over Swept Wings

PI: Demetri Telionis (telionis@vt.edu)
VA Tech, Blacksburg VA 24060

AFOSR Project No: F49620-00-1-0335
Period: 7/1/00 to 3/31/01
Level of Funding: $19,980
VA Tech Project No 430871

Introduction

This is a very short abstract of the work performed on this project. A more extended report that includes most of the experimental results is attached as an Appendix to this abstract. This is essentially one AIAA paper that was presented at the AIAA meeting in January 2001and two papers that were submitted for presentation to the AIAA meeting in January 2002. We have heard form the meeting organizers that both have been accepted.

Short Description of the Results.

An experimental study of active control of fully separated flow over a symmetrical circular-arc airfoil at high angles of attack was performed. The experiments were carried out in a low-speed, open circuit wind tunnel. Angles of attack from 10 to 40 degrees were tested. Low-power input, unsteady excitation was applied to the leading or trailing edge shear layers. The actuation was provided by the periodic oscillation of a 4-percent-chord flap placed on the suction side of the airfoil and facing the sharp edge. Pressure measurements over the airfoil show that the control increased the normal force coefficient by up to 70%. The application of flow control on sharp-edged aircraft wings could lead to improved maneuverability, innovative flight control and weight reduction.

In the continuation of this effort the wing was swept at angles up to 45 degrees. The experiments were carried out in a low-speed, open-circuit wind tunnel. Angles of attack from 10 to 40 degrees were tested again. The actuation was provided by the periodic oscillation of a 4-percent-chord flap placed on the suction side of the airfoil and facing the sharp edge. Pressure measurements over the wing show that the control increased the normal force coefficient by up to 50%. But the effectiveness of the method decreased with the angle of sweep.
We also designed a jet mechanism appropriate for fitting as close as possible to the leading edge of a sharp-edged airfoil. This is essentially a wedge shown in Fig. 1. The actuation mechanism consists of two concentric cylinders. The inner cylinder contains sixteen 1/16" wide slots, eight on each side, which span the length of the 7/16"-inch diameter inner brass tube. The inner cylinder rotates about a fixed axis inside a fixed outer cylinder created by the machined wedge. The inner cylinder is a brass tube, free to rotate on five bronze oilite bushings. One bushing was machined to fit snuggly between

the brass tubing and the machined leading edge at mid-span. This was done to eliminate the possible warping of the tube during use.

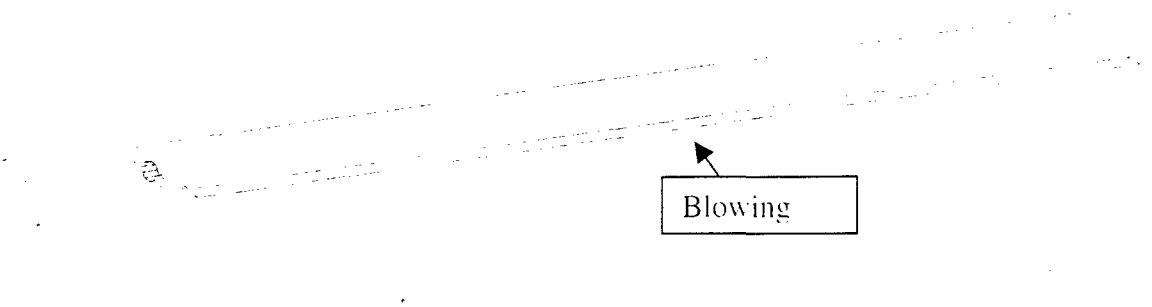

Figure 1: Machined Sharp Leading Edge with Flow Control Device

This device operates as follows. The inner tube is continuously supplied with high pressure air and is driven in rotation at a fixed frequency. When the slots of the inner rotating tube and the fixed outer tube match, the pressurized cavity releases air in the form of an unsteady jet. The flow is guided by the duct shown in Fig. 1 and released very close to the leading edge of the wedge. When the slots of the inner and the outer cylinder do not match, some air may leak between the two cylinders and find its way through the duct. We therefore anticipate that the unsteady jet will have a steady component on top of which an unsteady part will be superimposed. The terminology in this field has not yet been established but the jet thus created could be considered a synthetic jet, even though there is no suction on the jet nozzle. This is because the unsteady character of the flow will introduce the same nonlinear mechanism that will allow the jet to penetrate the outer flow.

The basic hypothesis here is that this device can produce pulsing jets with amplitudes independent of the driving frequency. To test this hypothesis, we measured the Pitot amplitudes at three locations along the span of the slot nozzle for a range of driving frequencies and for a fixed plenum pressure of 100 psi. The data indicate that the efficiency of the device is practically independent of the driving frequency.

Personnel.

Mr Matthew Zeiger worked on this project. Mr. Zeiger is an experineed student who just competed his Ph.D. work. This effort helped support him at the end of his studies at VA Tech. Mr. Zeiger helped train Ms. Gerlach and undergraduate student who will be entering our graduate program.

Publications.

1. "Flow Control of A Sharp-Edged Airfoil" by Sergio Miranda and Demetri P. TelionisMatthew P. Zeiger. Presented at the AIAA meeting in January, 2001.

2. "Flow Control of A Swept, Sharp-Edged Wing". By Matthew P. Zeiger, Jacquelynn Gerlach, Sergio Miranda and Demetri P. Telionis, accepted for presentation at the 2002 AIAA Aerospace Sciences Meeting.

3. "Frequency-and-Amplitude-Independent Flow Controller for Sharp-Edged Wings," by Matthew P. ZeigerJacquelynn M. Gerlach, Pavlos P. Vlachos and Demetri P. Telionis, accepted for presentation at the 2002 AIAA Aerospace Sciences Meeting.

Flow Control of A Sharp-Edged Airfoil

Sergio Miranda[1] and Demetri P. Telionis[2]
Department of Engineering Science and Mechanics
Virginia Polytechnic Institute and State University
Blacksburg, VA 24061

Matthew P. Zeiger[3,3]
Aerobrobe Corporation
Va Tech Corporate Research Center
Blacksburg, VA 24060

Abstract

An experimental study of active control of fully separated flow over a symmetrical circular-arc airfoil at high angles of attack was performed. The experiments were carried out in a low-speed, open circuit wind tunnel. Angles of attack from 10 to 40 degrees were tested. Low-power input, unsteady excitation was applied to the leading or trailing edge shear layers. The actuation was provided by the periodic oscillation of a 4-percent-chord flap placed on the suction side of the airfoil and facing the sharp edge. Pressure measurements over the airfoil show that the control increased the normal force coefficient by up to 70%. The application of flow control on sharp-edged aircraft wings could lead to improved maneuverability, innovative flight control and weight reduction.

Nomenclature

θ	Flap angle
L	Lift
ρ	Density
C_p	Pressure coefficient, $2(p-p_\infty)/\rho U_\infty^2$
C_n	Section normal force coefficient
U	Velocity
c	Airfoil chord length
f	Frequency
p	Pressure
α	Angle of attack
|F|	Reduced frequency $\equiv f_a / f_s$
|St|	Normalized Strouhal number $\equiv St / S_o$
$\|C_n\|$	Normalized section normal force coefficient $\equiv C_n / C_{n0}$

Subscripts:

stall	Static stall condition
∞	Free stream property
a	Actuator property
s	Shedding property
suc	Airfoil suction side
pres	Airfoil pressure side
0	Base case, no control applied.

Introduction

Over the past few decades, there has been a marked trend towards the design of fighter aircraft with low radar signature, capable of flying at supersonic speeds and maintaining high levels of maneuverability. Such requirements involve many physical and technical limitations, setting a new challenge to the industry.

Sharp edges are a common feature on these airframes, and separation can not be avoided for even low angles of attack. Flow control is a new approach in the design of new radical configurations. At moderate to high angles of attack, the suction side of the wings for low-observable fighter aircraft is dominated by separated flow that comprises of large and small vortices with a wide spectrum of length scales and frequencies.

Recent experimental and numerical evidence shows that at high angles of attack, it is possible to increase lift by as much as 70 percent, by controlling the vortex-forming process of separated flows. This can be achieved by utilizing low power actuators, effectively controlling the shear layer roll up over the wing. Indeed, for a wide range of angles of attack of wings with rounded leading edges, it has been shown

[1] Graduate Research Assistant
[2] Professor, Associate Fellow AIAA
[3] Senior Scientist

that many methods of micro-actuation are quite effective[1-4].

Attached flow can not be sustained over a sharp leading edge even at low angles of attack. Different means of flow control must be employed, i.e., flow control of separated flows. The only effort to control flow separating over a sharp leading edge is due to Zhu et al.[5]. These authors carried out some experiments with a rounded airfoil placed backwards in a wind tunnel, so that its sharp edge was leading. They only tested at an angle of attack of 27° but their results clearly indicated that increases in lift could be achieved.

Our goal is to be able to control the separated flow over a thin circular-arc airfoil. For that matter, we should clarify here the difference between separated flow control and flow separation control. Both imply the condition of a detached flow, but in a different flow scale. Fiedler[6] makes a clear distinction between these two flow fields. Weak separation can be defined as that one where the separation point location is variable or undefined. This is the case for most flow fields around rounded leading edge wings, where the separation point depends on the surface contour and flight condition.

The strong separation case is the one where the separation point is fixed. This applies to flows over sharp edges and to mostly all bluff bodies with sharp corners. The separation point is usually fixed at a sharp edge or corner. For both the strong and weak separation cases, passive and active controls are possible.

For rounded leading-edge airfoils, the weak or strong separation classification depends strictly on the angle of attack. Wu *et al.*[7] make a clear distinction between these two cases. For the angle of attack range $\alpha < \alpha_{stall}$, the flow is not fully separated, and control is aimed at overcoming separation. Usually the result is the complete elimination of the separated flow at a given α or the reattachment of the flow downstream, creating a recirculating bubble. For $\alpha > \alpha_{stall}$ the flow is fully separated, and it is most uncertain that the control will promote reattachment. This defines two control categories: *separation control* and *separated flow control*.

This research falls into the category of active control of strong separation, ie. separated flow control. The actuation is applied by means of an oscillating flap either on the leading or trailing edge.

Experimental Setup and equipment

Experiments were conducted in the Engineering Science and Mechanics wind tunnel. This is an open-circuit, low-speed tunnel, having a 5 to 1 contraction ratio and a test section measuring 0.51m by 0.51m and 1.27m in length. Freestream velocities range from 4 m/sec to 20 m/sec via an axial fan driven by a 5 hp dc motor. The generated velocities are very stable over time and the maximum turbulence intensity is 0.65%. The flow across the test section is reasonably uniform with a variation smaller than 1.5%.

An airfoil model with sharp leading and trailing edges was constructed. This is a symmetrical, circular-arc, 8-percent-chord thickness airfoil. The chord length is 0.2032 m (8 in) resulting in an airfoil maximum thickness of 0.0162 m (0.64 in). The model spans 0.5080 m (20 in), 2 mm less than the tunnel width. Endplates were employed to reduce the tunnel wall boundary layer detrimental effects.

A total of 61 pressure taps where installed on the airfoil, 30 on the suction side and 31 on the pressure side. A Pressure Systems Incorporated ESP Pressure Scanner is attached to the wall of the wind tunnel and used to measure the pressures over the airfoil. The Tygon tubing length is kept less than 30 cm, thus allowing a frequency response of about 50 Hz. The ESP pressure scanner utilized in the current research is a 32 Channel model with ±10 inches of water pressure range. When properly calibrated, the ESP has an accuracy of 0.10% of the full scale and an acceleration response of ±0.008% of full scale per g.

The actuation system consists of a flat plate of 4 percent airfoil chord length covering the entire model span as shown in Fig. 1. The thickness of the plate is

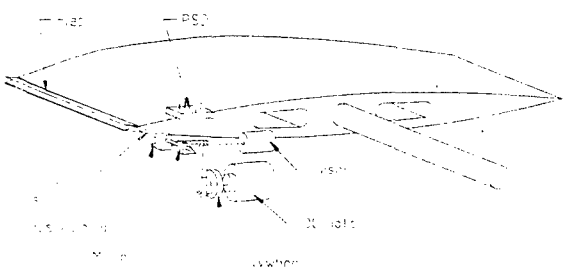

Fig. 1. The oscillating mechanism and laser positioning feedback mechanism.

0.127 mm (0.0050 in) and is made out of brass. The flat plate is attached at one of its ends to a 1.27 mm (0.05 in) diameter stainless steel rod, that works as the structural connection between the flap and the wing and at the same time allows the rotational movement of the flap. The rod is longer than the model span in order to link with the actuating mechanism from one side of the tunnel.

The flap is placed on one of the edges of the airfoil model. In its closed position, the flap edge coincides with one of the sides of the airfoil edges. The surface of the airfoil was countersank, so that in its parked position, the flap did not protrude above the surface of the airfoil nor did it extend over its edge. Since the airfoil model is symmetric, the flap can be placed on any side and edge for testing without having to change parts or disassembling the model. In this work, the flap was always placed on the suction side of the airfoil, and the chord position was changed between the leading edge and the trailing edge.

The flap is oscillated by a DC motor and an eccentric arrangement as shown schematically in Fig. 1. The motor shaft is connected to a flywheel equipped with an eccentric shaft. For the current research, the amplitude was fixed at 17, set with an accuracy of ±1°. The flywheel is balanced statically to work with minimum vibrations at speeds in the order of 100 Hertz.

An optical sensing system is employed to record and adjust the frequency of the flap oscillation. A position sensor detector (PSD) is used in conjunction with a laser pointer to give the exact position of the flap and its motion. The position sensing detectors are silicon photodiodes that provide an output directly proportional to the position of a light spot on the detector active area. For this research, the On-Trak Photonics 2L10-2 Duo-Lateral two-dimensional PSD is utilized.

The laser beam emanating from a laser pointer impinges on a small mirror attached on the flap-driving rod. As shown in Fig. 1, the reflected beam hits the PSD, which is positioned at an appropriate distance to allow the entire sensor photoelectric array to be used. In this way, knowing the set up geometry, a precise flap location can be given at any time. This system provides also a direct read-out of the flap frequency.

The most effective way of controlling the separated flow over the airfoil is by introducing disturbances with frequencies equal to the vortex shedding frequency and its harmonics. For this reason, a sensor is required to read a signal representative of the shedding activity. To this end, a Pitot rake was constructed, using high-frequency-response pressure transducers. The Pitot tubes capture the axial velocity variations in the wake of the airfoil, and the signals are digitally processed to obtain the required frequencies. The rake included six Pitot tubes, connected to six high-frequency Endevco Model 8510B-2 piezoelectric pressure transducers, with a 2 psig full range.

Four signal conditioning amplifiers are used, and the data are acquired by means of two A/D data acquisition boards on two computers. For the analog signal coming from the PSD, the Company's OT-300 position sensing amplifier is used. Signals from the six Endevcos are amplified and conditioned by Vishay Measurements Group Inc., Instrument Division, signal conditioning amplifier Model 2210. The six strain gage channels are amplified by Vishay Measurements Group Inc., Instruments Division, signal conditioning amplifier Model 2120A. For the multiplexed signal coming from the ESP, Aeroprobe's AP-2500 Box is utilized.

Two computers are employed for simultaneous data acquisition of airfoil pressure distribution, balance forces, and pressure rake survey. The arrangement of instrumentation is shown schematically in Fig. 2. Both computers are triggered externally through a simple LOW-HIGH triggering signal coming from a function generator. Computer I consists of a 166 MHz Intel Pentium processor and 32 MB of RAM memory. A RC Electronics ISC-16 board is employed for the analog-to-digital conversion. The ISC-16 is a 16 channel, 12 Bit, ±10 Volts range, capable of up to 1 MHz maximum rate.

The Hewlet-Packard HP-3562A Dynamic Signal Analyzer proved to be an important tool for the data acquisition process. Two channels are available for real time analysis of signals. The analyzer has functions attributed to oscilloscopes but also works as a real time digital signal processor, showing power spectrum densities, correlations, etc. This is a fundamental feedback tool to control and modify the vortex shedding phenomena, adjusting the actuator frequency, and observing changes in forces exerted on the balance. This reduces post-processing time by getting a real time feedback of the physics of the experiment.

Computer II is a 166 MHz Intel Pentium processor and 4 MB of RAM memory. The data acquisition board is a Computer Boards model CIO-DAS08-AOL, having an 8 channel, 20 kHz, programmable gain, and a two-channel 12-Bit digital to analog converter. Computer II is the platform for the Aeroprobe pressure measurement system. Proprietary software is utilized that controls all the required parameters on the ESP for calibration and data acquisition. The program is set for an external trigger, as done for Computer I. An Edwards-Datametrics Barocell precision pressure transducer converts the actual pressure to velocity, necessary to adjust the tunnel freestream velocity. It also takes part in the ESP static calibration, measuring the calibration pressures. The ESP is calibrated every 20 minutes, to maintain the required accuracy of the measurements.

Experimental Results

The flow is excited either at the leading edge or the trailing edge. In both cases the same flap mechanism is employed. The method of excitation of the shear layer was divided in two parts: perturbation

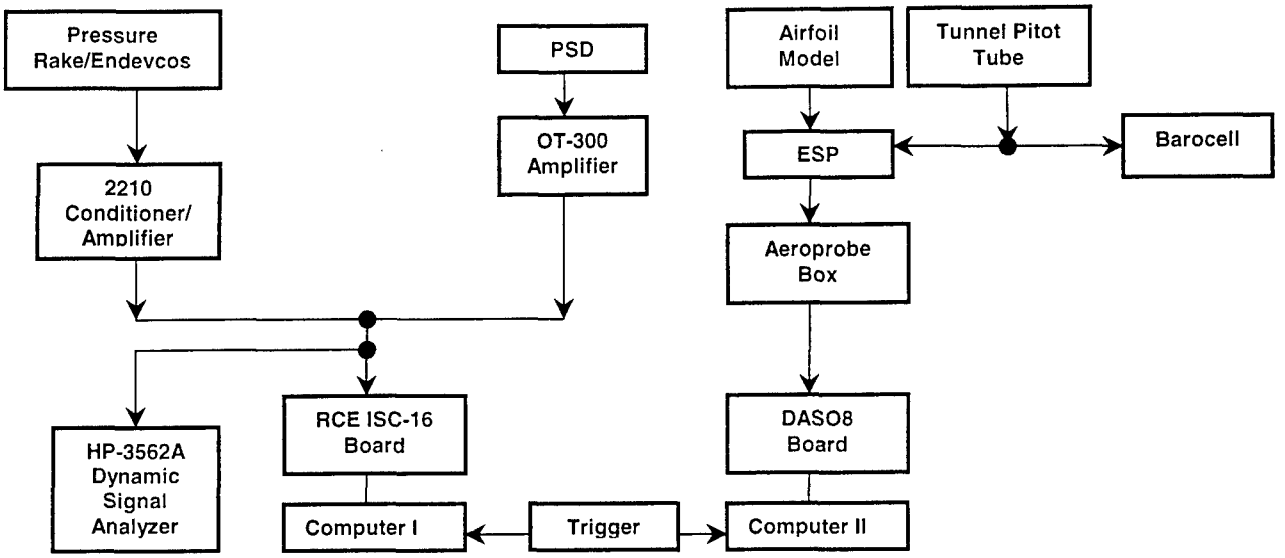

Fig. 2. Data acquisition system

of the leading edge shear layer and perturbation of the trailing edge shear layer. In both cases, we use the same flap set up. The difference lies in the rotation of the airfoil by an angle of (180 – 2 α) degrees from the desired angle of attack. The flap in both cases is located on the suction surface of the airfoil. If both vortex-vortex and sound-vortex resonance is present, this should be the best configuration, as suggested by Wu *et al*[8].

This research is a parametric study of the effects of the flap actuation for different angles of attack and different actuation frequencies. The following procedure was adopted:

I. Set the desired angle of attack.
II. Set the freestream velocity.
III. Using the HP signal analyzer, check the natural shedding frequency.
IV. Acquire data, no actuation applied.
V. Set excitation frequency.
VI. Acquire data with actuation.

This implies an iterative process. Steps V and VI are repeated until all possible/desired excitation frequencies are covered.

Experiments were conducted for the parameter values listed in Table 1. No effort was made to correct for tunnel blockage. The purpose here is to compare the actuated with the base flow.

Table 1. Matrix of experimental parameters.

Angle of attack	*Free-stream Velocity [m/sec]*	*Reynolds Number [x10^5]*	*Excita-tion Config-uration*	*Tunnel Blockage*
10°	17.5	2.22	LE	6.9%
15°	17.5	2.22	LE	10.3%
20°	17.5	2.22	LE/TE	13.7%
25°	17	2.16	LE	16.9%
30°	17	2.16	LE/TE	20%
40°	15.5	1.97	LE/TE	25.7%

1) Base flow results

In order to understand the fluid dynamics of the circular-arc airfoil at high angles of attack, results with no excitation are analyzed first. Pressure measurements taken over the surface of the airfoil are converted to pressure coefficients. The averaged values are displayed in Figure 3 for different angles of attack. It is important to note that a sensor malfunction is found in the port placed at the 62.3% of the chord on the suction side but the error appears to be consistent.

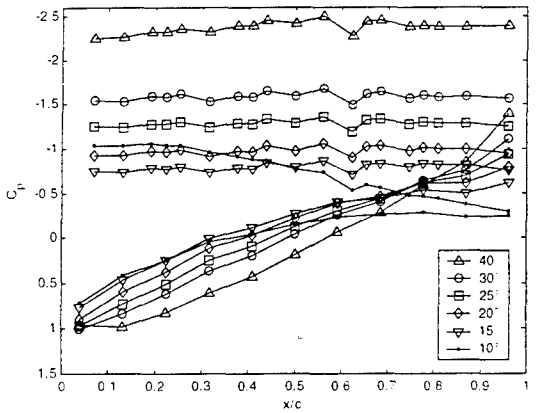

Fig. 3. Airfoil pressure coefficient distribution at different angles of attack. Suction and pressure sides. No actuation. For Reynolds number, see Table.

A clear constant offset out of the normal error margins is encountered for all cases.

The Figure shows a flat average pressure distribution on the suction side, for all angles of attack, except for the case of 10 degrees. This is typical for fully separated flows. This finding confirms the fact that for the flow over a sharp edged airfoil, separation is inevitable at the edges and reattachment is not possible, unless the airfoil is at low angles of attack. Indeed for $\alpha = 10°$, we observe that over the first half of the wing the pressure is again uniform but then in the aft half, there is a gradual increase. As the trailing edge is approached, the pressure coefficient of the two sides tend to a common value, signaling satisfaction of the Kutta condition. The stagnation point is very near to the leading edge except for the highest angle of attack. The point moves towards the leading edge as incidence is decreased.

Sensor No. 3 in the wake rake is chosent o monitor the flow in the wake of the model. The effect of change of angles of attack on the vortex shedding characteristics as detected by this sensor is represented in Figs. 4 and 5.

The vortical structure in the wake is characterized by two frequencies, a shedding frequency and also a component at the first harmonic. This is true for the high angles, whereas the second component reduces in magnitude as the angle of attack diminishes. For the 20° case, practically only one component is present.

The 15° case shows a less clear peak on the PSD plot, corresponding to a less organized flow. This could also imply that the flow is separated in the average, but a transient reattachment could exist due to the unsteadyness of the flowfield. A recirculating bubble is probably formed, periodically bursting and shedding

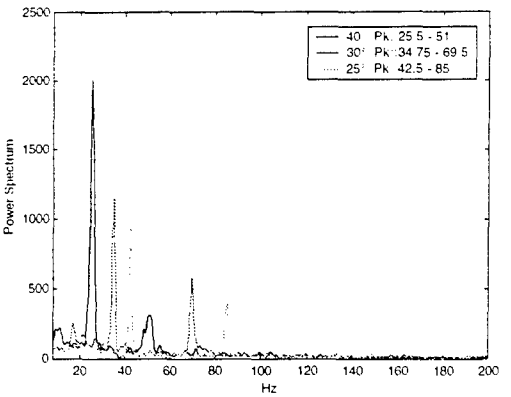

Fig. 4. PSD at angles 40° through 25°. Pitot 3. Reynolds number and freestream velocity as in Table 5.2.1. PK: peak values.

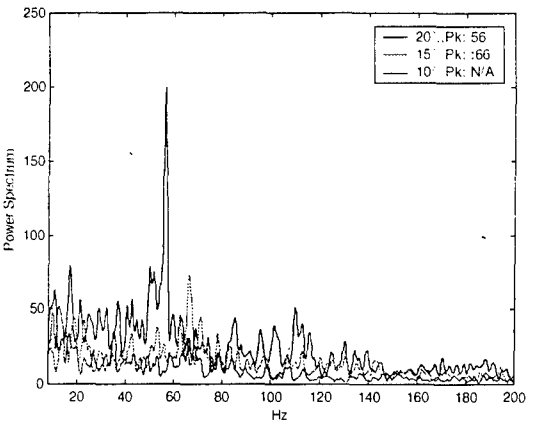

Fig. 5. PSD at angles 20° through 10°. Pitot 3. Reynolds number and free-stream velocity as in Table 5.2.1. PK: peak values.

away from the airfoil. For the 10° case, a peak is not present. Using the principle vortex shedding frequency, a Strouhal number can be computed, based on the frontal height of the airfoil:

$$St = \frac{f_s \, c \sin\alpha}{U_\infty} \qquad (1)$$

where f_s is the shedding frequency, c is the chordlength and α is the angle of attack and U_∞ is the free-stream velocity. This number was found to be between 0.2 and 0.22 for all angles of attack greater than 10°. Assuming the same Strouhal number, the shedding frequency for the 10° angle of attack should be in the neighborhood of 100 to 110 Hz.

2) Controlled Case

As previously mentioned, the data for different excitations were acquired by applying a disturbance at

frequencies around the corresponding natural frequency of vortex shedding for each angle of attack and freestream velocity. All data, were post-processed and compared with the base case for each angle of attack. Since flow over a sharp-edged bluff body maintains a small dependency on the Reynolds number, the effects can be extrapolated to configurations of engineering importance.

Both normal force coefficient and Strouhal number are calculated for the different excitation cases and normalized with respect to the base case, denoted by |Cn| and |St| respectively. Frequencies are reduced with the natural shedding frequency for the case under consideration. The results are plotted against reduced frequency |F| for each angle of attack in Figs. 6 through 11.

Many interesting conclusions can be drawn from these figures. The post-processed data can be divided into two categories with respect to the actuation effectiveness. One is the 'higher' angle of attack regime: 25, 30 and 40 degrees; and the other is the 'lower' angle of attack regime: 20, 15 and 10 degrees. Lift increases in the higher angle of attack regime are not as pronounced. Only a 10 percent increase is achieved in the best case for both the 40° and 25° angles, whereas in the 30° case there is very little evidence of any effect on the lift. This is quite disappointing, but expected from the predictions of Wu *et al* [6], who state that the angle of attack can not be too close to the stall angle nor could it have large values. At the same time, it is interesting to note that the trailing edge actuation results contradict the predictions of the same authors on the most effective placement of the excitation source, at least for the higher angles regime. The leading edge shear layer control, should be the best actuation due to the upstream location and the high receptivity. This is probably true only for the angle of attack range that they refer to. In the current results, the trailing edge flap gives for the 30° case the only source of lift increment. It is possible that an oscillating flap at the trailing edge but on the suction side may not be reaching the trailing edge shear layer. The last arguments presented in this paragraph then will not be valid.

Both 30° and 40° cases show also a very interesting behavior. As the experiment was repeated to confirm the repeatability of the results, a notable dispersion of the data was observed. This source of dispersion cannot be attributed to measuring errors. We believe that this behavior is due to a hysteresis phenomenon.

Transition from the higher to the lower angles of attack seems to be in the proximity of 20° to 25° angle of attack. There is no frequency at which a clear improvement in lift can be realized. A net increase, although small, can be seen for the 25° case on the reduced frequency equal to 1. Normalized Strouhal number analysis shows no effective frequency changes due to actuation. For the angle of attack of 40°, no changes are seen whatsoever. This leads us to conclude that the strong natural vortical structure is not affected by the excitation. It is also possible that at such angles of attack, the micro-flap is well within the separated region and could not affect the free shear layer. This is definitely valid in the case of trailing edge actuation.

Figure 7b shows shedding frequency shifting to the first harmonic or the subharmonic of the uncontrolled vortex shedding. The results in Fig. 17b are more affected by the excitation frequency, with shifting to the subharmonic values of the natural shedding frequency, some locking-on to harmonic of the excitation frequency, and the rest remain at low shedding frequencies relative to the base case.

In Figs. 9 through 11, we observe that the shedding frequency is locked on to the driving frequency for a wide range of frequencies. The very small disturbance introduced at the leading edge is enough to force the wake vortices to shed at driving frequency. This is clearly indicated by the fact that the data fall along a line inclined by 45°.

Figures 12 and 13 show the PSD for two cases, one for a 30°-angle of attack, and the other for a 25°-angle of attack. For both cases, a frequency lock-on takes place, but with different effects. In Figure 21 it can be seen that the excitation frequency organizes the vortical structure, locking the vortex shedding to the actuator frequency. Magnitude levels are overall lower, implying that the vortex structure is weaker than in the base flow. The second figure is even more interesting. Not only the shedding locks on to this new value, but the vortical formation is completely destroyed into a broader spectrum of vortices. This is the opposite of the desired goal.

Results for the 'lower' angles of attack are completely different to those of the 'higher'. Not only the excitation effect is effective, but also lift increments of up to 73% are achieved. This can be seen in Figure 19a for the15° angle of attack.

The fluid flow excitation at the 20° (Fig. 9) angle of attack shows a particular behavior in the normal force coefficient for each actuation frequency of the flap. In the range of the reduced frequency from 0 to 1, the normal force coefficient increases almost linearly, with a small peak located at the subharmonic of the natural shedding frequency, and reaching a maximum of 30% increase at the harmonic. Normal force increase is accompanied by a frequency lock-on starting at |F|=0.4 and continuing until |F|=1.13, as shown in Figure 9b. The normalized normal force coefficient has a maximum of around 25% increase between the range

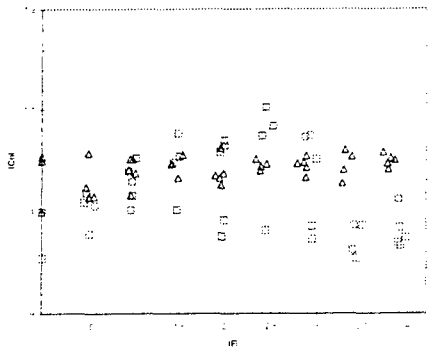

Fig. 6a. Normal force coefficient variation with excitation frequency. Angle of attack: 40°; □ leading edge flap actuation; △ trailing edge flap actuation.

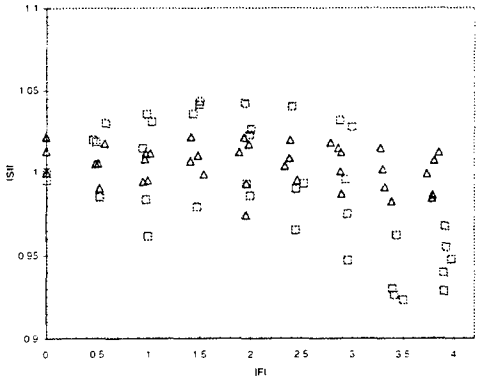

Fig. 6b. Strouhal number variation with excitation frequency. Angle of attack: 40°; □ leading edge flap actuation; △ trailing edge actuation.

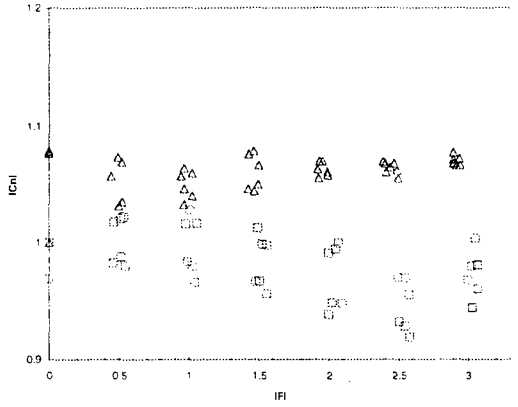

Fig. 7a. Normal force coefficient variation with excitation frequency. Angle of attack: 30°; □ leading edge flap actuation; △ trailing edge flap actuation.

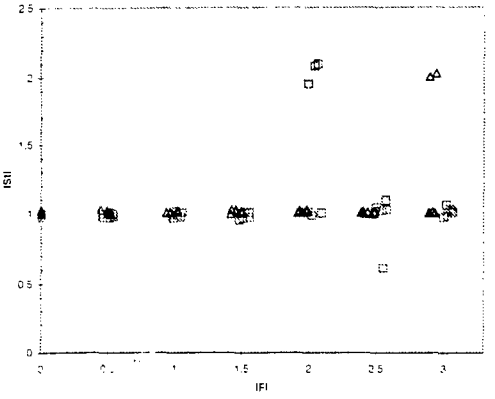

Fig. 7b. Strouhal number variation with excitation frequency. Angle of attack: 30°; □ leading edge flap actuation; △ trailing edge flap actuation.

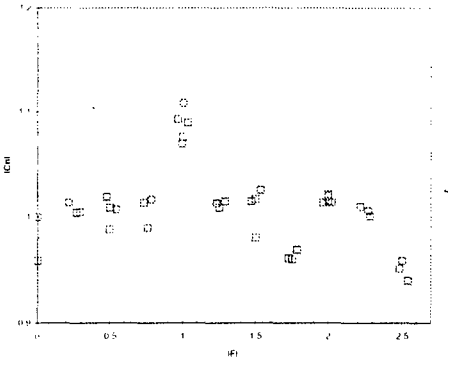

Fig. 8a. Normal force coefficient variation with excitation frequency. Angle of attack: 25°; leading edge flap actuation.

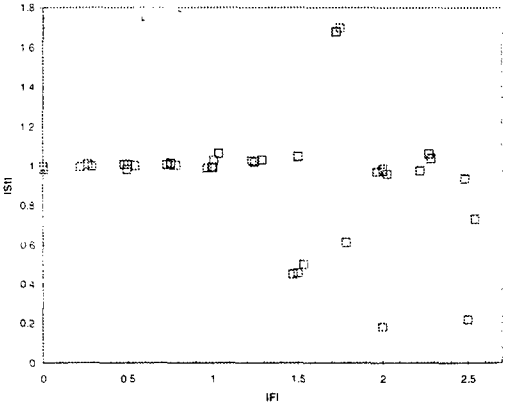

Fig. 8b. Strouhal number variation with excitation frequency. Angle of attack: 25°; leading edge flap actuation.

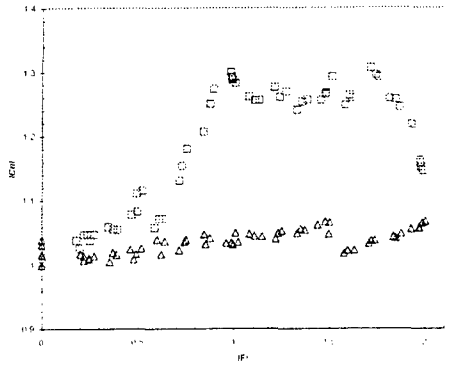

Fig. 9a. Normal force coefficient variation with excitation frequency. Angle of attack: 20°; _ leading edge flap actuation; △ trailing edge flap actuation.

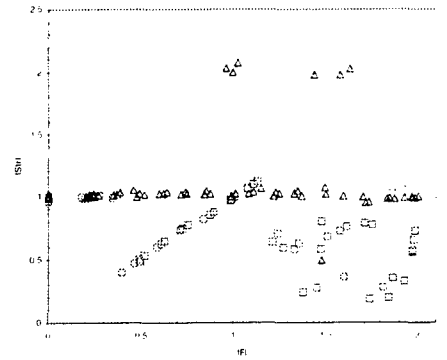

Fig. 9b. Strouhal number variation with excitation frequency. Angle of attack: 20°; _ leading edge flap actuation; △ trailing edge flap actuation.

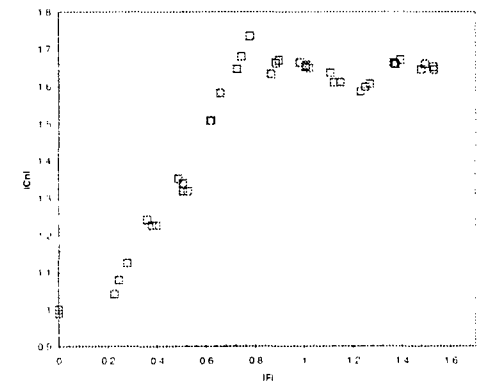

Fig. 10a. Normal force coefficient variation with excitation frequency. Angle of attack: 15°; leading edge flap actuation.

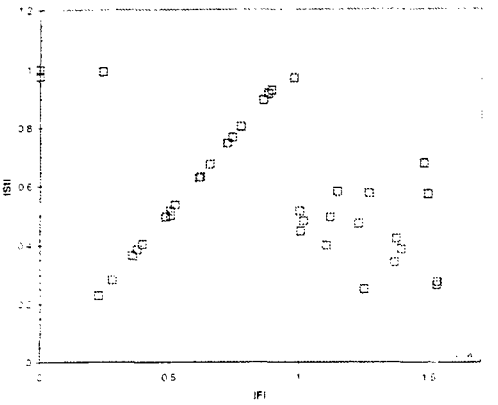

Fig. 10b. Strouhal number variation with excitation frequency. Angle of attack: 15°; leading edge flap actuation.

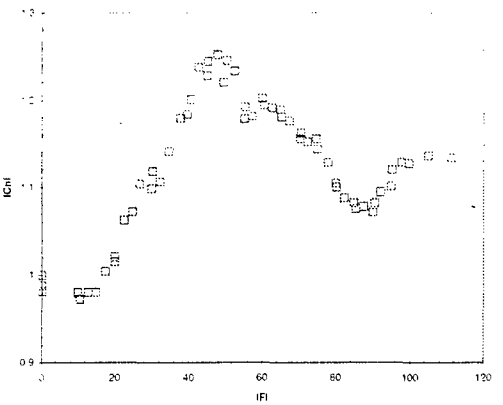

Fig. 11a. Normal force coefficient variation with excitation frequency. Angle of attack: 10°;leading edge flap actuation.

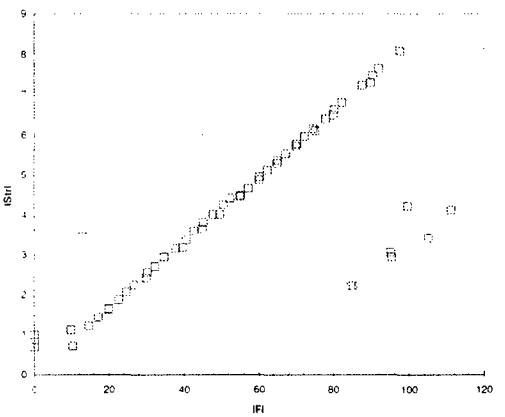

Fig. 11b. Strouhal number variation with excitation frequency. Angle of attack: 10°; leading edge flap actuation.

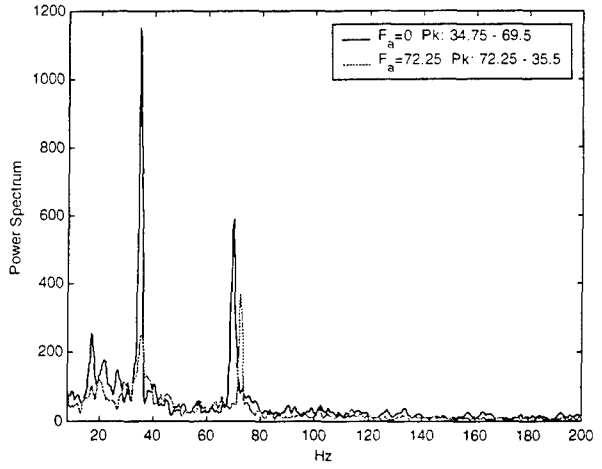

Fig. 12. PSD of pitot 3 at excitation |F|=2.06. Angle of attack 30°

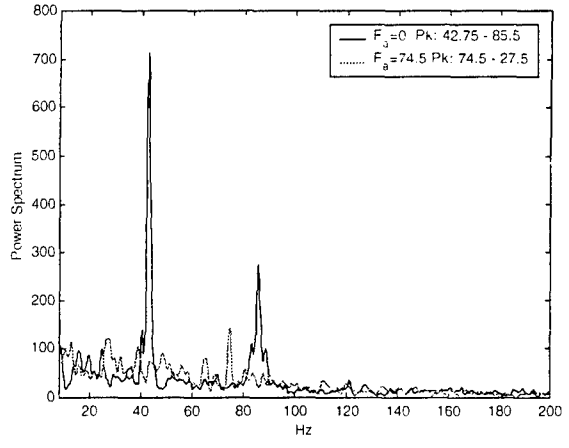

Fig. 13. PSD of pitot 3 at excitation |F|=1.75. Angle of attack 25°. Pk: peaks.

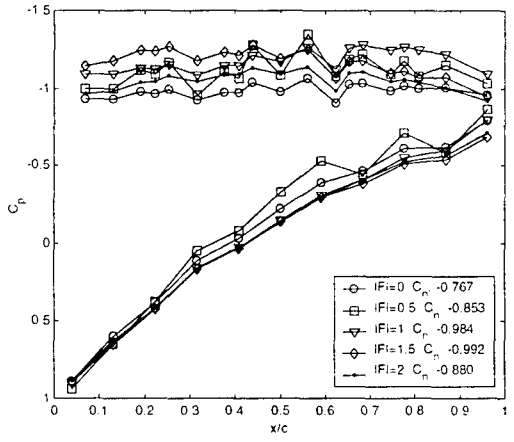

Fig. 14. Pressure coefficient distribution for controlled case. Angle of attack 20°. Leading edge excitation.

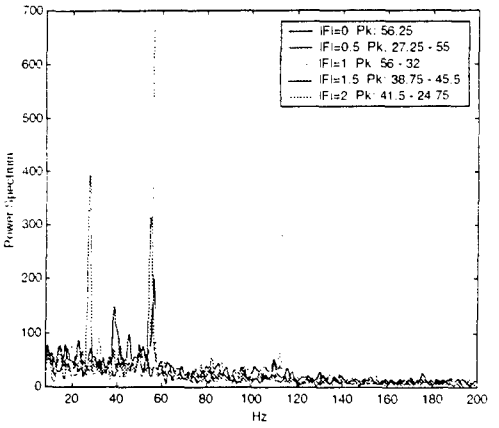

Fig. 15. PSD of pitot 3 for controlled case. Angle of attack 20°. Leading edge excitation.

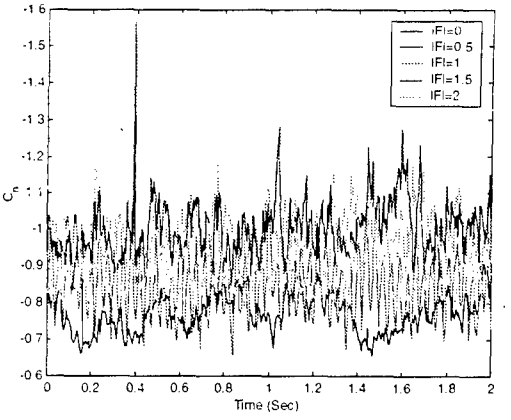

Fig. 16. Evolution of normal force coefficient for different actuation frequencies. Angle of attack 20°. Leading edge excitation.

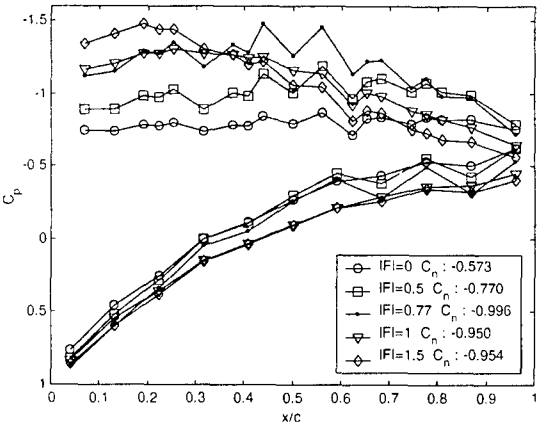

Fig. 17. Pressure coefficient distribution for controlled case. Angle of attack 15°. Leading edge excitation.

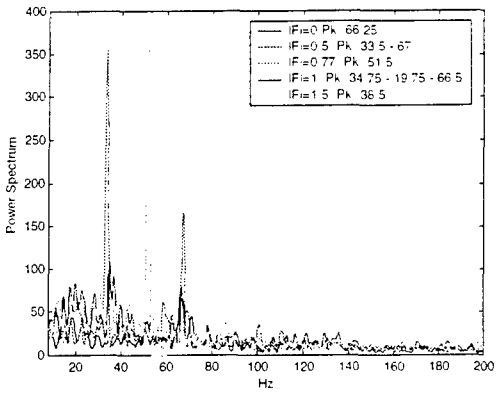

Fig. 18. PSD of pitot 3 for controlled case. Angle of attack 15°. Leading edge excitation.

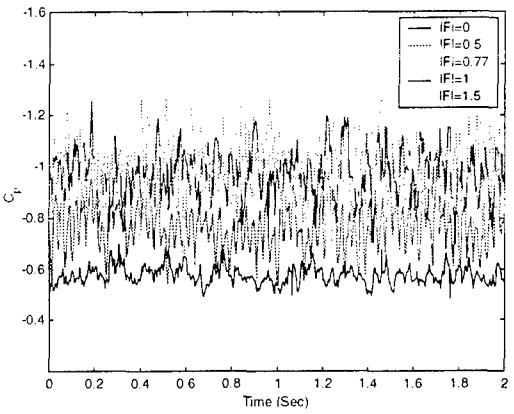

Fig. 19. Evolution of normal force coefficient for different actuation frequencies. Angle of attack 15°. Leading edge excitation.

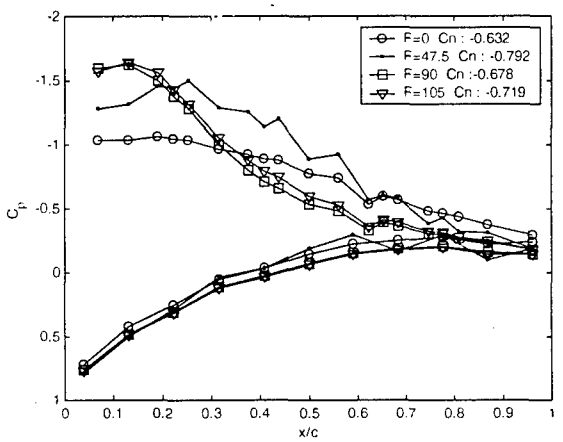

Fig. 20. Pressure coefficient distribution for controlled case. Angle of attack 10°. Leading edge excitation.

of 1 through 1.75 of |F|, dropping sharply for values beyond. The Strouhal number after the lock-on region drops to a value of around 0.5, showing a radical change in the vortex shedding pattern.

The pressure coefficient distribution over the airfoil at α = 20° is shown in Figure 14, and the corresponding PSD plot in Figure 15. Figure 14 shows that both values of reduced frequency 1 and 1.5 promote the same lift increment, but with a difference in the vortex structure on the suction side of the airfoil. The pressure distribution on the suction side of the latter is slightly higher for the first 50% of the chord and drops towards the trailing edge. The excitation at the natural shedding frequency behaves in the opposite way. The C_p increases slightly towards the trailing edge. This implies that a different mode of vortex formation is promoted, with the latter being formed towards the trailing edge. This effect has an important implication on the moment coefficient of the airfoil. A change in excitation frequency can shift the position of the aerodynamic center while retaining the magnitude.

It is also important to note how the overall change in circulation due to lift augmentation is being reflected in the pressure side, by shifting the pressure coefficient somewhat downwards.

Power spectra from the Pitot No. 3 in the wake, for α = 20° are shown in Fig. 15. The excitation at the natural frequency of the vortex shedding organizes the flow structure in its resonant mode. Coherent structures are formed as detected by the narrow band peaks on the fundamental frequency and close to subharmonic and first harmonic. The case for |F|=1.5 corresponds to a completely different level of flow structure. The peaks are not so clear, indicating a less organized flow. This might be even beneficial if the pressure oscillation levels are reduced by avoiding bigger vortices to be shed. That would be the ideal, namely maintain a big vortex in the average over the airfoil suction side, but shed smaller vortices at a higher frequency. To demonstrate this effect, we plotted in Fig. 16 the evolution of the normal force coefficient with time for the different excitation levels. No specific conclusion can be drawn from this figure, but it appears that all excitation frequencies seem to magnify the pressure oscillation levels.

The reduced flap frequency set at the subharmonic shedding frequency affects the airfoil pressure distribution in a particular mode. Various C_p peaks imply a dense vortical structure on the suction side. As seen in Figure 15 the flow is coherent, with two main frequencies governing the vortex organization. This could be related to two unstable vortices forming on the suction side and alternately shedding. This 'duality' forces the pressure distribution to oscillate more dramatically, as shown in Figure 16.

Trailing edge flap actuation does not affect the flow considerably, with a maximum lift augmentation of 6% at |F|=1.5 and repeated at |F|=2, not shown here due to lack of space. Vortex shedding is not modified unless for the reduced frequencies of 1 and 1.5, where the vortices seem likely to shed also at the subharmonic and first harmonic of the natural shedding values.

The 15° angle of attack generates the maximum lift increase on the airfoil, obtaining a 73% lift increment for a reduced frequency of about 0.75, as shown in Figure 20a. The encouraging fact is that lift increases linearly from the lowest reduced flap frequency tested to the most efficient one. This linearity may be useful if control of an aircraft is desired. After its highest value, the normal force coefficient settles at an average value of 1.63, showing some slight variations with flap frequency. The Strouhal number plot in Figure 20b shows that the linear increase is accompanied with a perfect frequency lock-on to the excitation frequency. This lock-on phenomenon extends up to the frequency of natural vortex shedding. Beyond this value, the shedding frequency drops to an average of the subharmonic value.

Figures 17 through 19 show the behavior of the relevant parameters with actuation frequency for the 15° case. As can be seen from the pressure distribution over the airfoil, reduced frequencies 0.5 and 0.77 lead to raising of the suction side pressure distribution, i.e. increasing lift. Lower pressure values in the middle of the chord indicate that a vortex positioned at half the chord of the airfoil gains strength with the excitation levels. The remarkable fact is evidence that the flow tends to reattach close to the trailing edge. This fact can be seen by simply extrapolating the measured values for both the suction and pressure side, and checking that the Kutta condition is satisfied. For the higher actuation frequencies, |F|=1 and |F|=1.5 the behavior found in the 20° case is also observed. For |F|=1 there is a tendency for spreading the pressure distribution along the extent of the chord, whereas for |F|=1.5 a suction peak at about x/c 0.2 develops. Both |F|=1 and |F|=1.5 induce a pressure side pressure increase.

Looking at the PSD plot in Fig. 18, that for the optimum frequency, a very coherent flow is achieved. A very narrow band frequency implies an organized vortical structure on the suction side of the airfoil, and the magnitude indicates a strong enhanced vortex. It is of interest to note that the frequency at which the vortex is enhanced is not related to the natural shedding frequency. For the subharmonic excitation, the subharmonic and the natural shedding frequencies are visibly enforced. The higher excitation frequencies do not organize the flow as the ones discussed so far. The frequency spectrum for the latter has broader peaks and low magnitudes. Figure 19 indicates again the trend seen for higher angles of attack, that when lift increases are obtained, the oscillation amplitude increases too.

For the smaller angle of attack, 10°, a different behavior of the flow control over the circular-arc airfoil is observed as shown in Fig. 9a. As mentioned before, this case did not show a natural shedding frequency. The calculated one should lie around 100 ~ 110 Hz. As control is applied, the effect found on the normalized normal force coefficient is similar to that of the 15° case. The difference is that |Cnl increases with frequency until a maximum of 25%, but then steadily decreases to a value of 7%. Then, a new increase of the normal force occurs and settles at 15%. This strange nonlinear behavior could be explained from the Strouhal number plot. It's clear that a perfect frequency lock-on is enforced on the shedding frequency. That frequency lock-on is extended until a maximum frequency of around 95~97 Hz is reached. This is close to the predicted (extrapolated) shedding frequency. This is not really a coincidence. The changes in the trends of |Cnl, i.e. increasing or decreasing values, occur at the subharmonic or the natural frequency. If we assume that 95~97 Hz is the natural shedding frequency, then the most efficient point occurs at the subharmonic frequency of shedding. Similarly, the second increase of lift settles down to a maximum at around the uncontrolled predicted shedding frequency. This implies that at 10° incidence the flow requires a perturbation to trigger the shedding of the vortices on the suction side of the airfoil.

Normal force coefficient increments are not as impressive as for the 15° case, but overall lift is augmented. Figures 20 and 22 show the effects of excitation in this particular case. It can be seen that the only frequency that really triggers the shedding phenomenon is that of the predicted subharmonic flap frequency. This appears clearly from the PSD plot in Figure 21. The lock-on frequency is evident, but also a component at twice that frequency, namely the estimated natural vortex shedding. For the other excitation values, the flow structure is not enhanced, as can be seen from the broad frequency spectrum.

Pressure distributions are also unexpected and unusual. While the highest reduced frequencies seem to promote reattachment of the flow, the optimum reduced frequency creates a vortex in the average sense over the suction surface, that increases further the suction force. This can be seen in Figure 20. Flow is reattached also in the average sense, but at a further downstream point. The plot of the airfoil pressure coefficient with respect to time, shows again that excitation increases oscillation amplitude.

It's interesting to remark that the classical thinking of the improvement of separated flow by forcing reattachment, does not necessarily mean that it will generate the largest lift (case |F|=47.5). If periodic

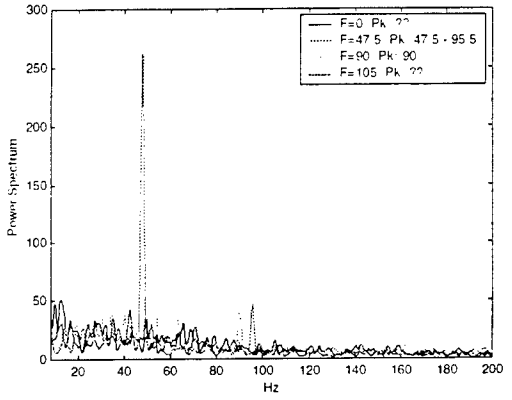

Fig. 21. PSD of pitot 3 for controlled case. Angle of attack 10°. Leading edge excitation.

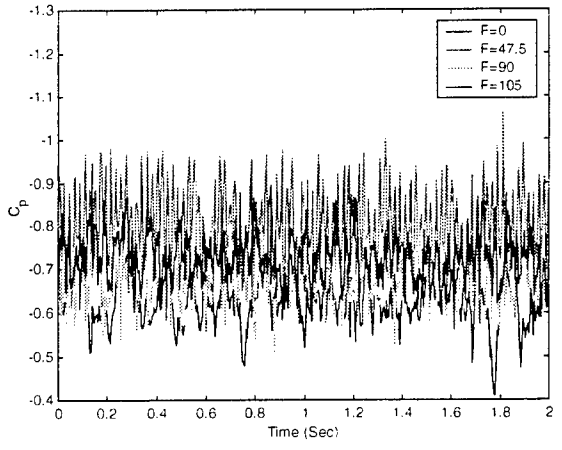

Fig. 22. Evolution of normal force coefficient for different actuation frequencies. Angle of attack 10°. Leading edge excitation.

excitation is applied, it is possible to capture a large vortex in the average and therefore provide even more lift than the fully attached flow case.

Conclusions.

We demonstrated experimentally that separated flow over sharp-edged airfoils could be managed by introducing small periodic disturbances at the leading or trailing edge. Unlike most other studies, we control here not the location of separation but separated flow itself. In other words, we accept the fact that massive separation exists and we try to modify it to our benefit. Our results indicate that lift could be increased in the average by as much as 70%

In our study we employed a large number of disturbing frequencies and proved that the flow control phenomenon under consideration is robust. The shedding events lock on to the externally introduced disturbance for a wide range of actuation frequencies. This means that the control mechanism could be relied upon to achieve increases of lift without the need of precisely matching the natural shedding frequency.

We found that the mechanism employed is effective for angles of attack up to 20 degrees. Very small increases in lift were found for angles of attack equal to 25, 30 and 40. Most interesting is the fact that even at an angle of attack of 10 degrees, for which no coherent wake oscillation is possible, actuation can reduce drastically the extent of the separated region, as detected by the suction side pressure distribution, which resembles more the distribution corresponding to attached flow. Driven at higher frequencies, there is evidence that a vortex is captured in the mean above the airfoil, because the pressure distribution indicates a wide area of very low pressure.

Acknowledgement.

Work on this paper was initiated with the encouragement of Prof. J.Z.Wu. Since then, the Air Force Office of Scientific Research provided support for this effort under Grant No. AFOSR #F49620-00-1-0335, Dr Steven Walker monitor.

References

1. Hsiao, F. –B., Liu, C. -F., Shyu, J. –Y., 1990,"Control of Wall-Separated Flow by Internal Acoustic Excitation", *AIAA Journal*, Vol. 28, No. 8, pp.1440-1446.
2. Hsiao, F. –B., Shyu, R. –N., Chang, R. C., 1994, "High Angle-of-Attack Airfoil Performance Improvement by Internal Acoustic Excitation", *AIAA Journal*, Vol. 32, No. 3, pp. 655-657.
3. Hsiao, F. –B., Wang, T.-Z., Zohar, Y., 1993, "Flow separation Control of a 2-D Airfoil by a Leading-Edge Oscillating Flap", Intl. Conf. Aerospace Sci. Tech., Dec. 6-9, 1993. Tainan, Taiwan.
4. Chang, R. C., Hsiao, F. –B., Shyu, R. –N., 1992, "Forcing Level Effects of Internal Acoustic Excitation on the Improvement of Airfoil Performance", *J. of Aircraft*, Vol. 29, No. 5, pp. 823-829.
5. Zhou, M. D., Fernholz, H. H., Ma, H. Y., Wu, J. Z., Wu, J. M., 1993, "Vortex Capture by a Two-Dimensional Airfoil with a Small Oscillating Leading-Edge Flap", AIAA 93-3266.
6. Fiedler, H. E., 1998, "Control of Free Turbulent Shear Flows", In *Flow Control: Fundamentals and Practices* (ed. Gad-el-Hak, M., Pollard, A., Bonnet, J. P.), pp. 335-429, Springer Lecture Notes in Physics, New Series Monographs, M53, Springer-Verlag, Berlin.
7. Wu, J. Z., Lu, X. Y., Denny, A. G., Fan, M., Wu, J. M., 1998, "Post-stall flow control on an airfoil by local unsteady forcing", *Journal of Fluid Mechanics* 371, pp. 21-58.
8. Wu, J. Z., Vakili, A. D., Wu, J. M., 1991, "Review of the Physics of Enhancing Vortex Lift by Unsteady Excitation", *Prog. Aerospace Sci.*, Vol. 28, pp. 73-131.

Flow Control of A Swept, Sharp-Edged Wing.

Matthew P. Zeiger[1,3]
Aerobrobe Corporation
Va Tech Corporate Research Center
Blacksburg, VA 24060

Jacquelynn Gerlach, Sergio Miranda[2] and Demetri P. Telionis[3]
Department of Engineering Science and Mechanics
Virginia Polytechnic Institute and State University
Blacksburg, VA 24061

Abstract

An experimental study of active control of fully separated flow over a symmetrical circular-arc wing at high angles of attack was performed. The wing was swept at angles up to 45 degrees. The experiments were carried out in a low-speed, open-circuit wind tunnel. Angles of attack from 10 to 40 degrees were tested. The actuation was provided by the periodic oscillation of a 4-percent-chord flap placed on the suction side of the airfoil and facing the sharp edge. Pressure measurements over the wing show that the control increased the normal force coefficient by up to 50%. But the effectiveness of the method decreased with the angle of sweep. The application of flow control on sharp-edged aircraft wings could lead to improved maneuverability, innovative flight control and aircraft weight reduction.

Nomenclature

θ	Flap angle
L	Lift
ρ	Density
C_p	Pressure coefficient, $2(p - p_\infty)/\rho U_\infty^2$
C_n	Section normal force coefficient
U	Velocity
	Airfoil chord length
	Frequency
	Pressure
	Angle of attack
$\|F\|$	Reduced frequency, $\equiv f c / U_\infty$

[1] Senior Scientist
Graduate Research Assistant
Professor, Associate Fellow AIAA

$\|St\|$	Normalized Strouhal number $\equiv St / S_o$
$\|C_n\|$	Normalized section normal force coefficient $\equiv C_n \; C_{n0}$

Subscripts:

stall	Static stall condition
∞	Free stream property
a	Actuator property
s	Shedding property
suc	Airfoil suction side
pres	Airfoil pressure side
0	Base case, no control applied.

Introduction

Sharp edges are a common feature on fighter aircraft with low radar signature, capable of flying at supersonic speeds and maintaining high levels of maneuverability. At moderate to high angles of attack, the suction side of the wings of such aircraft is dominated by separated flow that comprises of large and small vortices with a wide spectrum of length scales and frequencies. Flow control can be employed to improve the performance of such wings.

Recent experimental and numerical evidence shows that at high angles of attack, it is possible to increase lift by as much as 70 percent, by controlling the vortex-forming process of separated flows. This can be achieved by utilizing low power actuators, effectively controlling the shear layer roll-up over the wing. Indeed, for a wide range of angles of attack of wings with rounded leading edges, it has been shown that many methods of micro-actuation are quite effective[1-4].

Attached flow cannot be sustained over a sharp leading edge even at low angles of attack. Different means of flow control must be employed, i.e., flow control of separated flows. Zhu et al.[5] were the first to attempt controlling flow separating over a sharp leading edge. These authors carried out experiments with a rounded airfoil placed backwards in a wind tunnel, so that its sharp edge was leading. They only tested at an angle of attack of 27° but their results clearly indicated that increases in lift could be achieved.

The present group of investigators[6] carried out tests with a sharp-edged airfoil, controlling the flow with a miniature leading–edge flap. We should clarify here the difference between separated flow control and flow separation control. Both imply the condition of a detached flow, but in a different flow scale. Fiedler[7] makes a clear distinction between two flow fields. Weak separation can be defined as that one where the separation point location is variable or undefined. This is the case for most flow fields around rounded leading edge wings, where the separation point depends on the surface contour and flight condition.

The strong separation case is the one where the separation point is fixed. This applies to flows over sharp edges and to mostly all bluff bodies with sharp corners. The separation point is

usually fixed at a sharp edge or corner. For both the strong and weak separation cases, passive and active controls are possible.

For rounded leading-edge airfoils, the weak or strong separation classification depends strictly on the angle of attack. Wu *et al.*[8] make a clear distinction between these two cases. For the angle of attack range $\alpha < \alpha_{stall}$, the flow is not fully separated, and control is aimed at overcoming separation. Usually the result is the complete elimination of the separated flow at a given α or the reattachment of the flow downstream, creating a recirculating bubble. For $\alpha > \alpha_{stall}$ the flow is fully separated, and it is most uncertain that the control will promote reattachment. This defines two control categories: *separation control* and *separated flow control.*

This research falls into the category of active control of strong separation, ie. separated flow control. The actuation is applied by means of an oscillating flap either on the leading or trailing edge. The present investigators[6] demonstrated that significant increases of lift can be obtained by control of separated flow. In the present paper, we extend this work by examining the effect of sweeping a sharp-edged wing. There is some overlap with Ref. 6, because we found it necessary to describe again the model and the experimental rig.

Experimental Setup and equipment

Experiments were conducted in the Engineering Science and Mechanics wind tunnel. This is an open-circuit, low-speed tunnel, having a 5 to 1 contraction ratio and a test section measuring 0.51m by 0.51m and 1.27m in length. Free-stream velocities range from 4 m/sec to 20 m/sec via an axial fan driven by a 5 hp dc motor. The generated velocities are very stable over time and the maximum turbulence intensity is 0.65%. The flow across the test section is reasonably uniform with a variation smaller than 1.5%.

The airfoil model with sharp leading and trailing edges employed in the work, described in Ref. 6 was used again. This is a symmetrical, circular-arc, 8-percent-chord thickness airfoil. The chord length is 0.2032 m (8 in) resulting in an airfoil maximum thickness of 0.0162 m (0.64 in). The model spans 0.5080 m (20 in), 2 mm less than the tunnel width. To place this wing at different sweep angles, it was necessary to construct extensions, so that the swept wing always spanned the entire width of the tunnel.

A total of 61 pressure taps are distributed over the mid section of the wing, 30 on the suction side and 31 on the pressure side. A Pressure Systems Incorporated ESP pressure canner is attached to the wall of the wind tunnel and used to measure the pressures over the airfoil. The Tygon tubing length is kept less than 30 cm, thus allowing a frequency response of about 50 Hz. The ESP pressure scanner utilized in the current research is a 32 Channel model with ±10 inches of water pressure range. When properly calibrated, the ESP has an accuracy of 0.10% of the full scale and an acceleration response of ±0.008% of full scale per g.

The actuation system consists of a flat plate of 4 percent airfoil chord length covering the entire model span as shown in Fig. 1. The thickness of the plate is 0.127 mm (0.0050 in) and is made out of brass. The flat plate is attached at one of its ends to a 1.27 mm (0.05 in) diameter

stainless steel rod that works as the structural connection between the flap and the wing and at the same time allows the rotational movement of the flap. The rod is longer than the model span in order to link with the actuating mechanism from one side of the tunnel.

The flap is placed on one of the edges of the airfoil model. In its closed position, the flap edge coincides with one of the sides of the airfoil edges. The surface of the airfoil was countersank, so that in its parked position, the flap did not protrude above the surface of the airfoil nor did it extend over its edge. Since the airfoil model is symmetric, the flap can be placed on any side for testing without having to change parts or disassembling the model. In this work, the flap was always placed on the suction side of the airfoil, and the chord position was changed between the leading edge and the trailing edge.

The flap is oscillated by a DC motor and an eccentric arrangement as shown schematically in Fig. 1. The motor shaft is connected to a flywheel equipped with an eccentric shaft. For the current research, the amplitude was fixed at 17°, set with an accuracy of ±1°. The flywheel is balanced statically to work with minimum vibrations at speeds in the order of 100 Hertz.

An optical sensing system is employed to record and adjust the frequency of the flap oscillation. A position sensor detector (PSD) is used in conjunction with a laser pointer to give the exact position of the flap and its motion. The position sensing detectors are silicon photodiodes that provide an output directly proportional to the position of a light spot on the detector active area. For this research, the On-Trak Photonics 2L10-2 Duo-Lateral two-dimensional PSD is utilized.

The laser beam emanating from a laser pointer impinges on a small mirror attached on the flap-driving rod. As shown in Fig. 1, the reflected beam hits the PSD, which is positioned at an appropriate distance to allow the entire sensor photoelectric array to be used. In this way, knowing the set up geometry, a precise flap location can be given at any time. This system provides also a direct read-out of the flap frequency.

The most effective way of controlling the separated flow over the airfoil is by introducing disturbances with frequencies equal to the vortex shedding frequency and its harmonics. For this reason, a sensor is required to read a signal representative of the shedding activity. To this end, a Pitot rake was constructed, using high-frequency-response pressure transducers. The Pitot tubes capture the axial velocity variations in the wake of the airfoil, and the signals are digitally processed to obtain the required frequencies. The rake included six Pitot tubes, connected to six high-frequency Endevco Model 8510B-2 piezoelectric pressure transducers, with a 2 psig full range.

Four signal conditioning amplifiers are used, and the data are acquired by means of two A/D data acquisition boards on two computers. For the analog signal coming from the PSD, the Company's OT-300 position sensing amplifier is used. Signals from the six Endevcos are amplified and conditioned by Vishay Measurements Group Inc., Instrument Division, signal conditioning amplifier Model 2210. The six strain gage channels are amplified by Vishay Measurements Group Inc., Instruments Division, signal conditioning amplifier Model 2120A. For the multiplexed signal coming from the ESP, Aeroprobe's AP-2500 Box is utilized.

Two computers are employed for simultaneous data acquisition of airfoil pressure distribution, balance forces, and pressure rake survey. The arrangement of instrumentation is shown schematically in Fig. 2. Both computers are triggered externally through a simple LOW-HIGH triggering signal coming from a function generator. Computer I consists of a 166 MHz Intel Pentium processor and 32 MB of RAM memory. A RC Electronics ISC-16 board is employed for the analog-to-digital conversion. The ISC-16 is a 16 channel, 12 Bit, ±10 Volts range, capable of up to 1 MHz maximum rate.

The Hewlet-Packard HP-3562A Dynamic Signal Analyzer proved to be an important tool for the data acquisition process. Two channels are available for real time analysis of signals. The analyzer has functions attributed to oscilloscopes but also works as a real time digital signal processor, showing power spectrum densities, correlations, etc. This is a fundamental feedback tool to control and modify the vortex shedding phenomena, adjusting the actuator frequency, and observing changes in forces exerted on the balance. This reduces post-processing time by getting a real time feedback of the physics of the experiment.

Computer II is a 166 MHz Intel Pentium processor and 4 MB of RAM memory. The data acquisition board is a Computer Boards model CIO-DAS08-AOL, having an 8 channel, 20 kHz, programmable gain, and a two-channel 12-Bit digital to analog converter. Computer II is the platform for the Aeroprobe pressure measurement system. Proprietary software is utilized that controls all the required parameters on the ESP for calibration and data acquisition. The program is set for an external trigger, as done for Computer I. An Edwards-Datametrics Barocell precision pressure transducer converts the actual pressure to velocity, necessary to adjust the tunnel free-stream velocity. It also takes part in the ESP static calibration, measuring the calibration pressures. The ESP is calibrated every 20 minutes, to maintain the required accuracy of the measurements.

Experimental Results

This research is a parametric study of the effects of the flap actuation for different angles of attack and different actuation frequencies. The following procedure was adopted. For each sweep angle:

I. Set the desired angle of attack.
II. Set the free-stream velocity.
III. Using the HP signal analyzer, check the natural shedding frequency.
IV. Acquire data, no actuation applied.
V. Set excitation frequency.
VI. Acquire data with actuation.

This implies an iterative process. Steps V and VI are repeated until all possible/desired excitation frequencies are covered.

1) Base flow results

In order to understand the fluid dynamics of the circular-arc airfoil at high angles of attack, results with no excitation are analyzed first. Pressure measurements taken over the surface of the airfoil are converted to pressure coefficients. The averaged values were reported inRef. 6 and are displayed again here in Figure 3 for different angles of attack. It is important to note that a sensor malfunction is found in the port placed at the 62.3% of the chord on the suction side but the error appears to be consistent. A clear constant offset out of the normal error margins is encountered for all cases.

The Figure shows a flat average pressure distribution on the suction side, for all angles of attack, except for the case of 10 degrees. This is typical for fully separated flows. This finding confirms the fact that for the flow over a sharp edged airfoil, separation is inevitable at the edges and reattachment is not possible, unless the airfoil is at low angles of attack. Indeed for $\alpha = 10°$, we observe that over the first half of the wing the pressure is again uniform but then in the aft half, there is a gradual increase. As the trailing edge is approached, the pressure coefficients of the two sides tend to a common value, signaling satisfaction of the Kutta condition. The stagnation point is very near to the leading edge except for the highest angle of attack. The point moves towards the leading edge as incidence is decreased.

2) Controlled flow results

Pressure data were averaged and and reduced to generated pressure coefficients. These data are plotted versus the chord distance for the pressure and the suction side of the wing. These are presented in Figs. 3 through 12. In all these figures, frame a represents the no-control case and frame b the controlled case. In Figs. 3 through 5, we present the data for a sweep angle of 10°and angles of attack of 15°,20° and 35°. We observe in these figures that the distribution of the pressu

ERROR: timeout
OFFENDING COMMAND: timeout

STACK:

Frequency-and-Amplitude-Independent Flow Controller for Sharp-Edged Wings

Matthew P. Zeiger[1]
Aerobrobe Corporation
Va Tech Corporate Research Center
Blacksburg, VA 24060

Jacquelynn M. Gerlach[2], Pavlos P. Vlachos[3] and Demetri P. Telionis[4]
Department of Engineering Science and Mechanics
Virginia Polytechnic Institute and State University
Blacksburg, VA 24061

Introduction

Many aviation applications such as military stealth fighters and supersonic transport aircraft require sharp edge configurations. Over the past few decades, the design of stealth fighters, capable of flying at supersonic speeds, and maintaining high maneuverability has been in great demand. Low radar detection dictated the use of flat surfaces and sharp edges. For supersonic transports, flying at high Mach numbers requires smaller, thinner, sharp-edged wings. These wings however are very inefficient in take-off and landing, requiring high speeds and long runways. The aerodynamic performance of sharp-edged wings is very poor at low speeds, because the flow separates over the leading edges, even at low angles of attack, with detrimental effects like increase in drag, decrease in lift, and reduction in aircraft maneuverability. Flow control may be an option and the present authors have demonstrated that indeed, this technique could improve the aerodynamics of sharp-edged wings (Miranda et al. 2001).

Flow control is defined as "the ability to actively or passively manipulate a flow field to effect a desired change" (Gad-el-Hak). Control of separated flow is possible by both passive and active means. Passive control would consist of changing the geometry

---

[1] Senior Scientist
[2] Student
[3] Visiting Assistant Professor, member AIAA
[4] Professor, Associate Fellow AIAA

of the aircraft to increase its aerodynamic properties. This type of control is unacceptable in the present case, due to stealth geometry and speed constraints. Active flow control must be used. The aim here is to control the flow that is already separated.

In order to create the necessary flow disturbance, a small oscillating flap can be placed on the leading edge of the wing. This pulsing flap creates an unsteady excitation at the leading edge, which is responsible for affecting the flow in the desired way. Previous work has demonstrated that the maximum effect on the flow is achieved when the actuation frequency is near the vortex shedding frequency. The flap must penetrate the separated region in order to have any effect on the formation of vortices.

Hsiao and Wang (1993) employed a pulsed micro-flap on the leading edge of a wing to control separated flow. They focused on the position, amplitude, and frequency of the flap motion necessary to improve the aerodynamics characteristics of the flow over an airfoil at high angles of attack. Hsiao and Wang found that periodic perturbations can organize and enhance the average strength of the shedding vortices and can increase in a time-average sense the lift by as much as 50%. Hsiao, et al. (1998) later made modifications to their previous design, finding that the most effective excitation corresponds to a flap motion with the vortex shedding frequency. They also found that larger amplitudes of excitation motion produced a larger lift coefficient.

A blowing technique has also been tested to control separated flow. Small jets are mounted at the leading edge of airfoils for the purpose of developing periodic perturbations into the boundary layer. The idea is to produce streamwise vortices using transverse steady and oscillating flow jets to increase the cross-stream mixing and lead to stall suppression in adverse pressure gradients. Several studies have been conducted on the use of oscillating blowing. McManus and Magill (1996) studied the separation control in incompressible and compressible flow using pulsed jets. They tested a NACA-4412 airfoil section with a leading edge flap. The leading edge flap was fitted with flow control actuators, each actuator consisted of a cross flow jet with pitch and screw angles of 90 and 45 degrees respectively. High-speed flow control valves were used to control

the pulsed flow to each jet individually. The leading edge contained three jet nozzles: however only two were used. The valve open-and-close cycle was manipulated using a computer function generator driving a solenoid valve power supply. The valve controller allowed pulse rates up to 500 Hz and volume flow rates in excess of 20 slugs/min for each jet. A constant average mass flow of air was supplied to the jet using a closed-loop servo valve. Their data indicated that maximum lift enhancements occur with a jet pulse Strouhal number of approximately 0.6. However, McManus and Magill found the pulsed jets caused an increase in lift of up to 50 percent over a base line case for $\alpha \leq 10$ degrees. It was found that the effectiveness decreased with the increase in Mach number. The best results were found when the angle of attack was equal to the angle corresponding to C_{lmax}.

Seifert, Bachar, Koss, Shepshelovich, and Wygnanski (1993) also examined oscillatory blowing . In their research a NACA-0015 airfoil with a trailing edge flap and jets mounted in a 2-D slot located on the upper surface above the hinge of the flap was used. It was placed at an angle of attack of 20 degrees. Seifert et al. concluded that steady blowing had no effect on lift or drag. However, modulating blowing generated an increase in lift and cut the drag in half.

Synthetic jet actuators based on cavity designs and driven by piezoelectric devices are most efficient at the resonance frequency of the piezo and limited by the natural frequency of the cavity. Such actuators have proven very useful in the laboratory but may not be as effective in practice. Oscillating flaps are not limited in their frequency domain. Indeed Miranda et al. (2001) have demonstrate that an oscillating flap can generate a wide range of effective frequencies for the control of separated flow over a sharp-edged wing. But such a devise may be not attractive for the aircraft designer. Recognizing these facts, Gilarranz and Rediniotis (2001) designed essentially a small positive-dispacement machine. They tested a NACA0015 wing with rounded leading edges containing six reciprocating compressors, which were driven by two DC motors. These compressors/pistons created a synthetic jet (zero mean flux) at the leading edge of the airfoil. They found that flow separation control was demonstrated at angles of attack and free stream velocities as high as 25° and 45 m/s, respectively

In the present paper we describe an alternative mechanism that would be uniformly effective in a large range of frequencies.

Actuator Design.

We designed a jet mechanism appropriate for fitting as close as possible to the leading edge of a sharp-edged airfoil. This is essentially a wedge shown in Fig. 1. The actuation mechanism consists of two concentric cylinders shown in Figure 2. The inner cylinder contains sixteen 1/16" wide slots, eight on each side, which span the length of the 7/16"-inch diameter inner brass tube. The inner cylinder rotates about a fixed axis inside a fixed outer cylinder created by the machined wedge. The inner cylinder is a brass tube, free to rotate on five bronze oilite bushings. One bushing was machined to fit snuggly between the brass tubing and the machined leading edge at mid-span. This was done to eliminate the possible warping of the tube during use. Two smaller bushings of the same type were placed in the inner brass tube. One was fixed to a pressure hose, so the cylinder could rotate independently of the fixed pressure line. The other was fixed to a motor drive shaft and the inner tube so that the inner cylinder can be driven by a small DC motor. The last two bushings are used to stabilize the tube in the machined leading edge but allowing rotation at the same time. All the bushings were press-fit to insure that the inner and outer cylinders are sealed tightly in order to maintain pressurization.

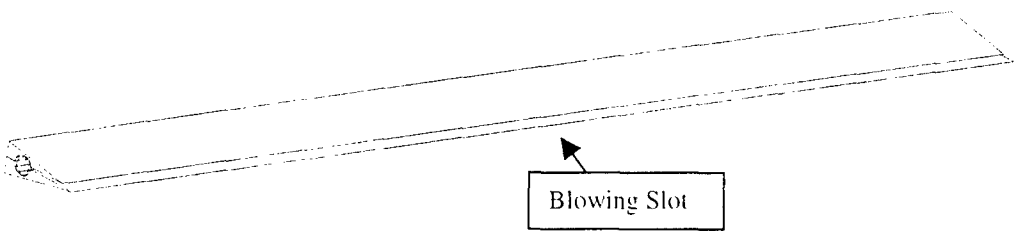

Figure 1: Machined Sharp Leading Edge with Flow Control Device

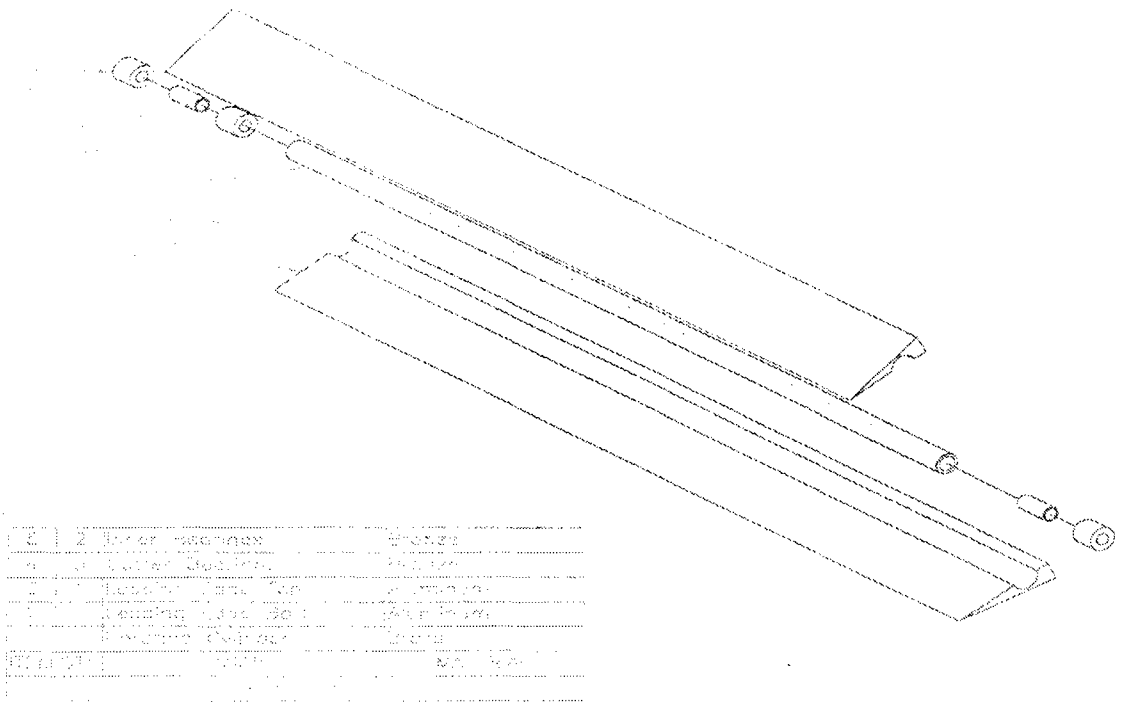

Figure 2: Exploded View of Flow Control Device

This device operates as follows. The inner tube is continuously supplied with high pressure air and is driven in rotation at a fixed frequency. In Figure 3 we show that inner cylinder slots away by 90 degrees with respect to the fixed slots. When the slots of the inner rotating tube and the fixed outer tube match, the pressurized cavity releases air in the form of an unsteady jet. The flow is guided by the duct shown in Fig. 3 and released very close to the leading edge of the wedge. When the slots of the inner and the outer cylinder do not match, some air may leak between the two cylinders and find its way through the duct. We therefore anticipate that the unsteady jet will have a seady component on top of which an unsteady part will be superimposed. The terminology in this field has not yet been established but the jet thus created could be considered a synthetic jet, even though there is no suction on the jet nozzle. This is because the unsteady character of the flow will introduce the same nonlinear mechanism that will allow the jet to penetrate the outer flow.

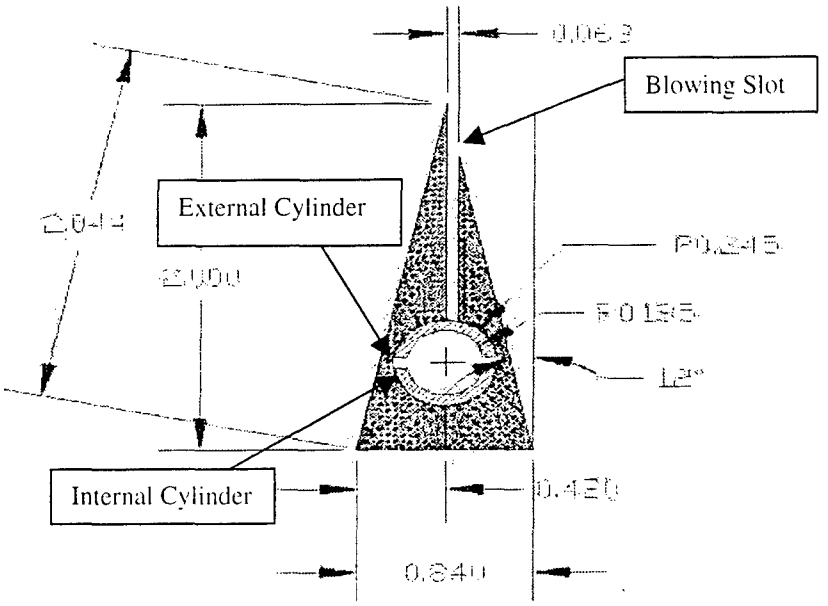

Figure 3: Cross Section of Flow Control Device

Testing

To test this design we mounted the assembled leading edge actuator in the test section of a wind tunnel aligned with a rake of four high-frequency-response Pitot tubes, as shown in Figure 4. The rake was connected to a HP digital signal analyzer, which was used to measure jet frequencies and amplitudes. It was mounted on three traversing scales so it could easily be displaced to obtain data at different locations downstream of the slotted nozzle.

A typical wave form of the Pitot signal obtained over the slotted nozzle is shown in Fig. 6. Power spectra of such signals revealed that the dominant frequency of the jet was the driving frequency of the motor. This confirmed that no motions were generated by nonlinear interactions and therefore, as anticipated, we could generate pulsing jets with the frequencies desired.

Figure 5: Leading Edge Aligned with Pitot Rake

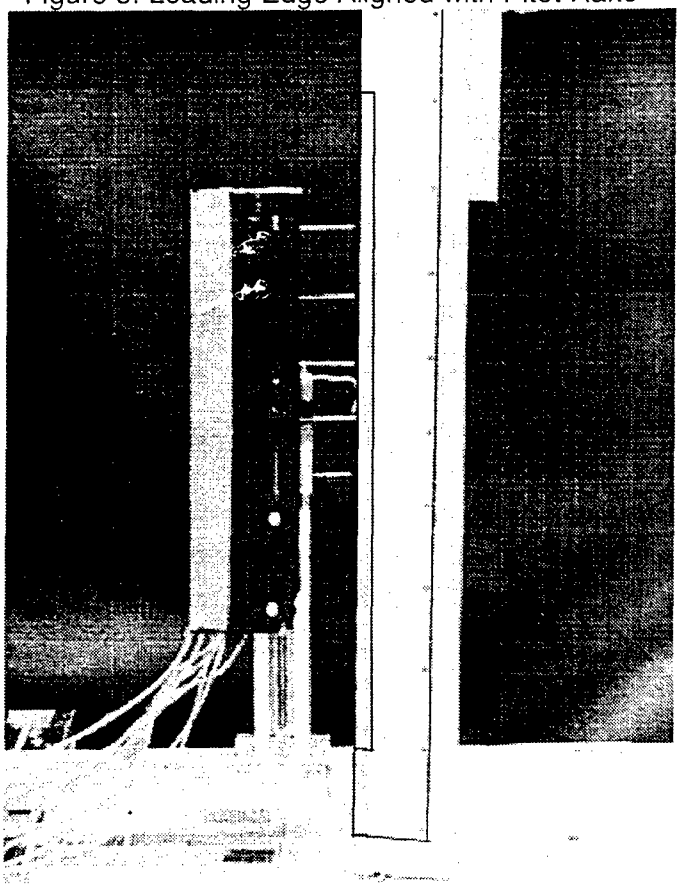

We tested the actuator at pressures ranging from 50psi to 120psi and frequencies between 40 and 120 Hertz. More evidence that the device could produce the desired frequency is displayed in Fig. 7 where we plot the jet frequency as a function of the plenum pressure. Apparently, the jet pulsing frequency is independent of the pressure.

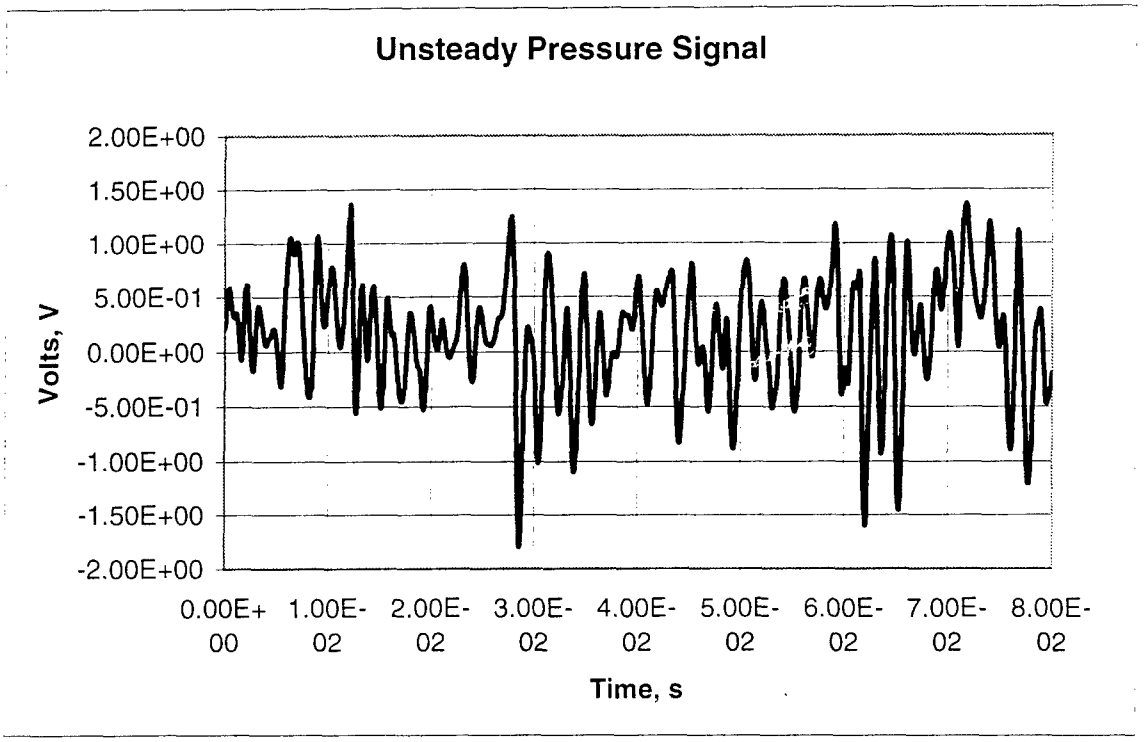

Fig. 6. Pressure time record.

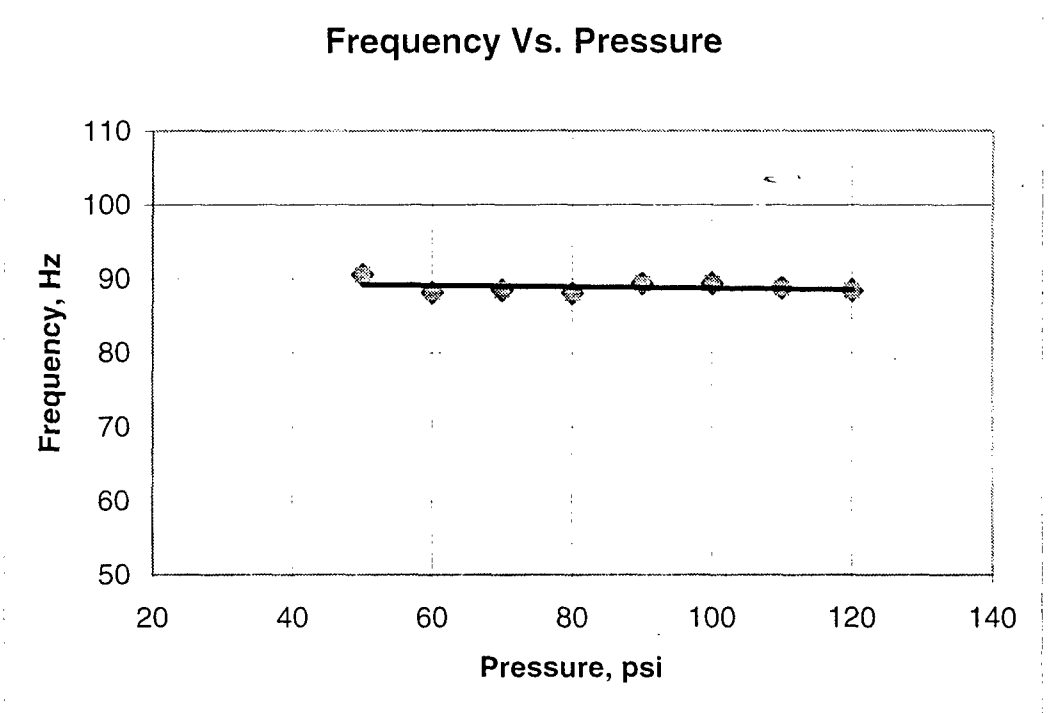

Figure 7: Frequency as a Function of Applied Pressure

The basic hypothesis here is that this device can produce pulsing jets with amplitudes independent of the driving frequency. To test this hypothesis, we measured the Pitot amplitudes at three locations along the span of the slot nozzle for a range of driving frequencies and for a fixed plenum pressure of 100 psi. The results are presented in Fig. 8. Pitot positions were numbered from the top down. These data indicate that the efficiency of the device is practically independent of the driving frequency. The data corresponding to position 2 indicate a very low amplitude but this is due to the fact that this probe found itself between two slots and therefore recorded no pulsing jet.

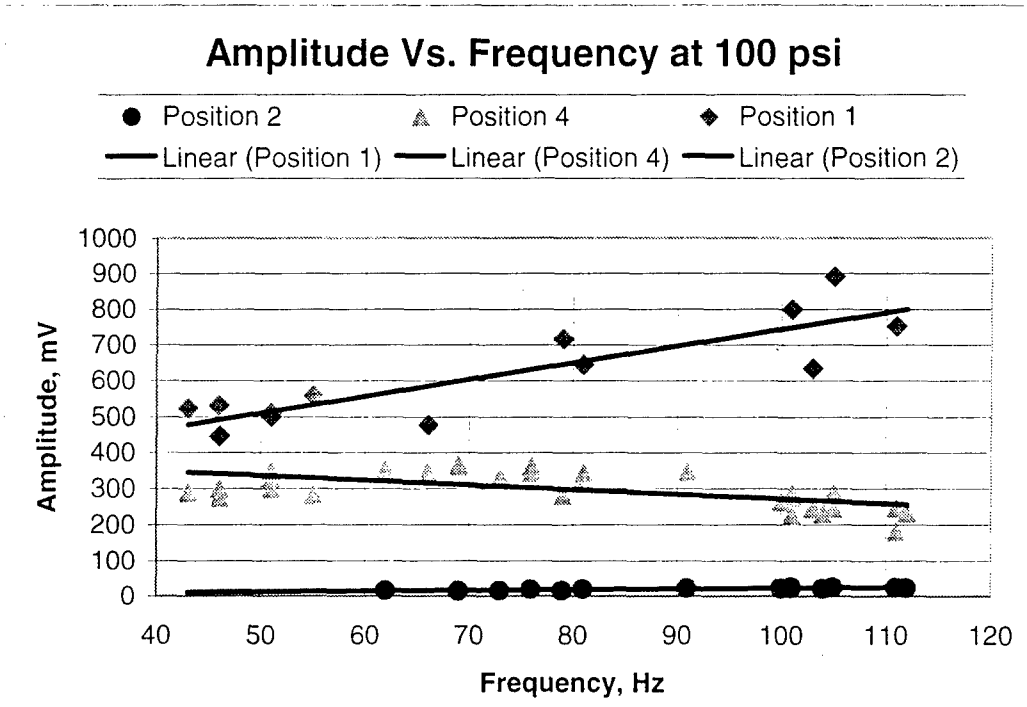

Figure 8 Amplitude as a Function of Frequency at 100psi

The amplitudes of the pulsing jets are increasing with the plenum pressure as shown in Fig. 9. This relationship appears to be monotonic, except for position 2 but as discussed before, the sensor at this position is placed in between two slots and therefore does not represent a free jet record.

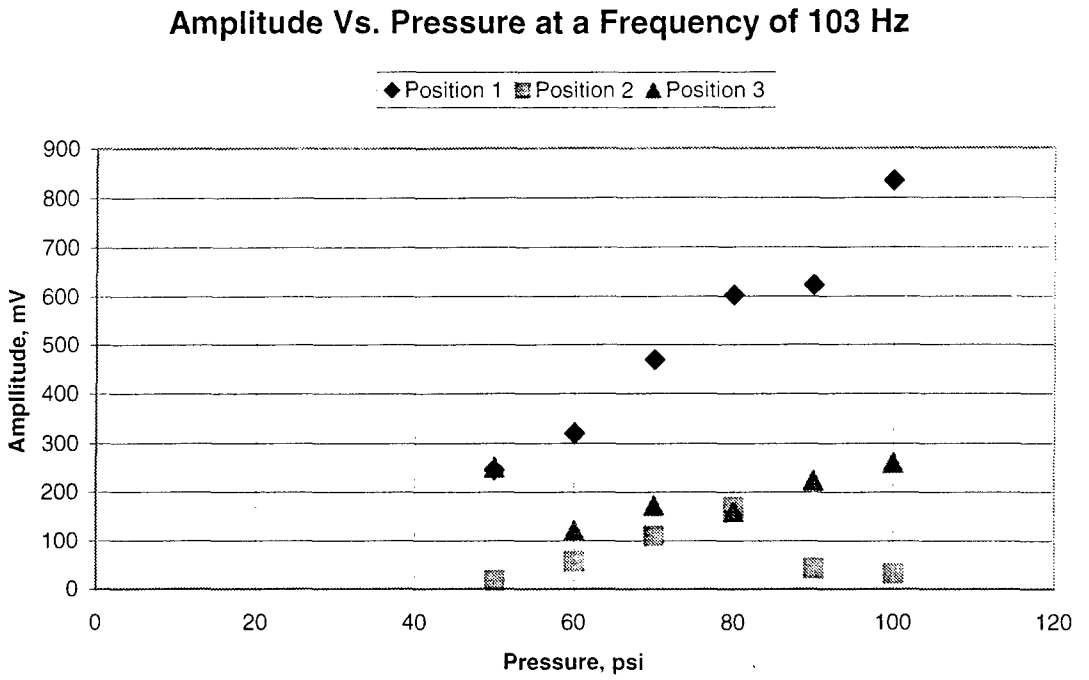

Figure 9 Amplitude as a Function of Applied Pressure at a Frequency of 103 Hz

We are presently taking more data with the Pitot rake by traversing the rake to document more carefully the distribution of the velocity of the pulsing jets. These data will be reduced to velocity distributions. We are also taking data with hot wires to confirm the validity of the data obtained with the high-frequency-response Pitot rake. Finally, we are in the process of obtaining PIV data along the same locations. These measurements are carried out with a CMOS digital camera that allows us to take over 5000 frames per second.

Conclusions:

We described in this paper an actuator that can generate a pulsing jet along a slotted nozzle. The basic feature of this device is that it can generate pulsing flow without any mechanical oscillating parts, like a pulsating wall or an oscillating piston. Another common limitation that the device can overcome is in the range of frequencies achieved. The pulsing jet frequency is controlled by the rotation of the inner cylinder and the number of the slots machined along its

circumference. The frequency of rotation of a well-balanced cylinder can be increased easily but more important is the fact that the pulse jet frequency is a multiple of the rotation frequency. The factor of the multiplicity is the number of the slots machined along the circumference. In the case presented here, there are two lines of slots, machined apart by 180 degrees and therefore the frequency of jet pulsing is double the motor frequency.

Our experimental data indicate that the efficiency of this actuator is practically independent of the frequency. This is means that the device is an excellent candidate for a robust flight actuator, where the required frequency is changing with aircraft speed and the angle of attack.

References:

I HAVE TWO SETS OF REFS. NEED TO SELECT THE CORRECT ONES

1. Gad-el-Hak, M., 1998, "Introduction to Flow Control." In Flow Control: Fundamentals and Practices (ed. Gad-el-Hak, M., Pollard, A., Bonnet, J. P.), pp. 1-107, Springer Lecture Notes in Physics, New Series Monographs, M53. Springer-Verlag, Berlin.
2. Gilarranz, J. L., Rediniotis, O. K., 2001, "Compact, High-Power Synthetic Jet Actuators For Flow Separation Control," AIAA Paper 2001-0737.
3. Hsiao, F. B., Liang, P. F., Huang, C. Y., 1998, "High-Incidence Airfoil Aerodynamics Improvement by Leading-edge Oscillating Flap," J. of Aircraft, Vol. 35, No. 3, pp. 508-510.
4. Hsiao, F. –B., Wang, T.-Z., Zohar, Y., 1993, "Flow separation Control of a 2-D Airfoil by a Leading-Edge Oscillating Flap," Intl. Conf. Aerospace Sci. Tech., Dec. 6-9, 1993, Tainan, Taiwan.
5. McManus, K., Magill, J., 1996, "Separation Control in Incompressible and Compressible Flows using Pulsed Jets," AIAA Paper 96-1948.

6. Miranda, S., Telionis, D., Zeiger, M., 2000, "Flow Control of a Sharp-Edged Airfoil," To be Presented at AIAA Conference in Jan. 2001.
7. Seifert, A., Bachar, T., Koss, D., Shepshelovich, M., Wygnanski, I., 1993, "Oscillatory Blowing: A Tool to Delay Boundary-Layer Separation," AIAA Journal, Vol. 31, No. 11, pp. 2052-2060.
8. Zhou, M. D., Fernholz, H. H. Ma, H. Y., Wu, J. Z., Wu, J. M., 1993, "Vortex Capture by a Two-Dimensional Airfoil with a Small Oscillating Leading-Edge Flap," AIAA Paper 93-3266.

References:

9. Gad-el-Hak, M., 1998, "Introduction to Flow Control." In Flow Control: Fundamentals and Practices (ed. Gad-el-Hak, M., Pollard, A., Bonnet, J. P.), pp. 1-107, Springer Lecture Notes in Physics, New Series Monographs, M53, Springer-Verlag, Berlin.
10. Gilarranz, J. L., Rediniotis, O. K., 2001, "Compact, High-Power Synthetic Jet Actuators For Flow Separation Control," AIAA Paper 2001-0737.
11. Hsiao, F. B., Liang, P. F., Huang, C. Y., 1998, "High-Incidence Airfoil Aerodynamics Improvement by Leading-edge Oscillating Flap," J. of Aircraft, Vol. 35, No. 3, pp. 508-510.
12. Hsiao, F. –B., Wang, T.-Z., Zohar, Y., 1993, "Flow separation Control of a 2-D Airfoil by a Leading-Edge Oscillating Flap," Intl. Conf. Aerospace Sci. Tech., Dec. 6-9, 1993, Tainan, Taiwan.
13. McManus, K., Magill, J., 1996, "Separation Control in Incompressible and Compressible Flows using Pulsed Jets," AIAA Paper 96-1948.
14. Miranda, S., Telionis, D., Zeiger, M., 2000, "Flow Control of a Sharp-Edged Airfoil," To be Presented at AIAA Conference in Jan. 2001.
15. Seifert, A., Bachar, T., Koss, D., Shepshelovich, M., Wygnanski, I., 1993, "Oscillatory Blowing: A Tool to Delay Boundary-Layer Separation," AIAA Journal, Vol. 31, No. 11, pp. 2052-2060.

16. Zhou, M. D., Fernholz, H. H., Ma, H. Y., Wu, J. Z., Wu, J. M., 1993, "Vortex Capture by a Two-Dimensional Airfoil with a Small Oscillating Leading-Edge Flap," AIAA Paper 93-3266.